

AD-A098 994

NAVAL RESEARCH LAB WASHINGTON DC
NUMERICAL STUDY OF SPACE CHARGE LIMITED TRANSPORT IN A QUADRUPOL--ETC(U)
MAY 81 I HABER
NRL-MR-4474

F/6 20/7

NL

UNCLASSIFIED

1 of 1
2 of 4
5094394

END
DATE
FILED
6 81
DTIC

AD A098994

REPORT DOCUMENTATION PAGE		READ INSTRUCTIONS BEFORE COMPLETING FORM
1. REPORT NUMBER NRL Memorandum Report 4474	2. GOVT ACCESSION NO. AD-A098994	3. RECIPIENT'S CATALOG NUMBER
4. TITLE (and Subtitle) NUMERICAL STUDY OF SPACE CHARGE LIMITED TRANSPORT IN A QUADRUPOLE TRANSPORT SYSTEM WITH 90 DEGREE PHASE ADVANCE	5. TYPE OF REPORT & PERIOD COVERED Interim report on a continuing NRL Problem	
7. AUTHOR(s) Irving Haber	6. PERFORMING ORG. REPORT NUMBER	
8. PERFORMING ORGANIZATION NAME AND ADDRESS Naval Research Laboratory Washington, DC 20375	9. CONTRACT OR GRANT NUMBER(s)	
11. CONTROLLING OFFICE NAME AND ADDRESS U.S. Department of Energy Washington, DC 20545	10. PROGRAM ELEMENT, PROJECT, TASK AREA & WORK UNIT NUMBERS 47-0898-0-1	
14. MONITORING AGENCY NAME & ADDRESS (if different from Controlling Office)	12. REPORT DATE May 21, 1981	
	13. NUMBER OF PAGES 46	
16. DISTRIBUTION STATEMENT (of this Report) Approved for public release; distribution unlimited.	15. SECURITY CLASS. (of this report) UNCLASSIFIED	
17. DISTRIBUTION STATEMENT (of the abstract entered in Block 20, if different from Report)	15a. DECLASSIFICATION/DOWNGRADING SCHEDULE	
18. SUPPLEMENTARY NOTES		
19. KEY WORDS (Continue on reverse side if necessary and identify by block number)		
Inertial confinement fusion Heavy ion fusion Accelerator technology Beam transport	Numerical simulation Particle simulation	
20. ABSTRACT (Continue on reverse side if necessary and identify by block number) Several computer simulations are described which examine the influence of space charge instabilities on an intense beam propagating down an alternate gradient focused channel. By following the detailed non-linear evolution of this system at various currents it is shown that instabilities can cause emittance growth which, by diluting the phase space density of the beam, can limit the current intensity which can be transported.		

DD FORM 1 JAN 73 1473

EDITION OF 1 NOV 68 IS OBSOLETE
S/N 0102-014-6601

SECURITY CLASSIFICATION OF THIS PAGE (When Data Entered)

CONTENTS

ADDENDUM	iv
I. INTRODUCTION	1
II. SIMULATION RESULTS	1
III. CONCLUSIONS	8
ACKNOWLEDGMENTS	10
REFERENCES	11
APPENDIX — Current Scaling in a Strong Focusing Channel	16

Accession For	
NTIS GRA&I	<input checked="" type="checkbox"/>
DLIC TAB	<input type="checkbox"/>
Unpublished	<input type="checkbox"/>
Justification	
Classification	
Control Codes	
Date Entered	
Initials	
A	

ADDENDUM

Propagation in a Transport System with 60 Degree Phase Advance.

The simulations described in this report were performed on an alternate gradient focusing system with a low current phase advance of 90 degrees per cell. In this case, the current intensity appears to be limited by space charge driven emittance growth. More recent results have shown that a transport system with a 60 degree phase advance behaves differently and the current does not appear to be similarly limited.

By considering the linear stability of a K-V distribution, Laslett and Smith [1] have determined that a 60 degree system can stably transport a more intense beam than a 90 degree system. Simulations similar to those described here were performed to verify that a K-V system, with a 60 degree phase advance depressed to 24 degrees by space charge, will propagate with no emittance growth or evidence of instability.

More recent simulations performed by Hofmann [2,3] on a 60 degree transport system found that a waterbag distribution with a depressed phase advance of 12 degrees showed no substantial rms emittance growth. Motivated by these results, simulations of a K-V distribution with depressed tunes of 12 degrees and 6 degrees were run. While the K-V distribution does show evidence of the theoretically predicted instabilities, the instability saturates at a very low level and rapidly approaches the squared distribution described by Hofmann. In contrast to the 90 degree system, very little rapid growth in the rms emittance is observed. Some very small slow growth in the rms emittance is observed, but after propagation through 100 magnet pairs the rms emittance has grown only about 5%. This absence of growth in the rms emittance is similar to what is observed in the simulation of continuously focused channels [3].

In summary, recent results have indicated that beam propagation in a 60 degree channel appears possible at much higher intensities than can be achieved in a 90 degree system.

REFERENCES

1. L.J. Laslett and Lloyd Smith, "Stability of Intense Transported Beams," IEEE Trans. on Nucl. Sci., NS26, p. 3090 (June, 1979).
2. I. Hofmann, "Emittance Growth of Ion Beams with Space Charge," presented at Conf. on Charged Particle Optics, Giessen, FRG, Sept. 1980.
3. I. Hofmann, "Emittance Growth of Beams Close to Space Charge Limit," IEEE Trans. on Nucl. Sci., NS28 (June, 1981).

NUMERICAL STUDY OF SPACE CHARGE LIMITED TRANSPORT IN A QUADRUPOLE TRANSPORT SYSTEM WITH 90 DEGREE PHASE ADVANCE

I. INTRODUCTION

The possibility of using a beam of energetic heavy ions to ignite an inertially confined thermonuclear pellet, [1,2] has increased the interest in transporting low emittance high current beams. It has been known for some time [3] that such beams are subject to space charge driven instabilities. Questions concerning the onset of these instabilities and their effect on beam transport have been the subject of a considerable body [3-9] of theoretical and computational study.

In this report, several computer simulations are presented which examine the influence of space charge driven instabilities on the behavior of a thin lens, alternate gradient, transport system with a 90 degree phase advance per cell. These simulations follow the evolution of several thousand simulation particles in their self consistent electric fields. By following the detailed non-linear evolution of this system at various current levels, it is shown that these space charge driven instabilities can cause emittance growth. The behavior is found to depend on the current. But the results, which show that increasing the current also increases the emittance growth, suggest that this emittance growth, by diluting the phase space density of the beam, may place an upper limit on the current intensity which can be transported.

In Section II we discuss the simulation results, and in Section III we discuss the implications to the transport of intense currents.

II. SIMULATION RESULTS

The behavior of quadrupole transport systems in the presence of space charge has been investigated for beams with Kapchinskij-Vladimirskij (K-V) distributions [11] by integrating the K-V envelope

equations [12,13]. Stability of K-V systems has in turn been investigated by a perturbation analysis of these envelope equation solutions [13-17]. Regions of rapid instability, with growth times of just several magnet traversals, have been discovered.

The envelope equation formalism has not, however, yielded insight into the saturation levels or the general non-linear behavior of these instabilities. When the amplitude of the unstable modes becomes large, the beam can no longer be approximated by a K-V distribution. Though envelope equations can be used under some circumstances to predict the behavior of non K-V systems [18,19], and some recent work has been done on instabilities in non K-V systems [20-22], even the linear behavior of these unstable systems is not yet understood. Previous simulations [23] have shown that for moderate tune depressions, the system evolves to a steady state after only a factor of two growth in emittance. The simulations presented here were performed in order to extend that work to a range of current intensities so as to systematically investigate the non-linear evolution of an unstable K-V system.

The numerical model is a two dimensional particle simulation code of the particle-in-cell type [24] optimized for a Texas Instruments ASC computer. The simulation is performed in a plane perpendicular to the direction of beam propagation, in a reference frame moving with the beam. All variation in the beam direction is neglected in this frame. Since the transverse behavior is nonrelativistic, velocities and momenta will be referred to interchangeably for notational convenience.

Numerical tests have been performed [25] which indicated the existence of a broad numerical regime where the simulation results are independent of numerical parameters. These tests showed that variations of such parameters as time step, grid size, boundary location, and number of particles by factors of two from the values used, left the results essentially unchanged. The simulations described here were generally performed on a 128×128 system employing 16384 simulation particles and using six time steps to follow the evolution from the center of one magnet to the center of the next. In order to eliminate the possibility that any emittance growth observed is due to numerical effects, a series of

simulations was also performed to test the dependence of emittance growth on the number of particles used in the simulation [26]. Care was used in all cases to ensure that the number of particles in the simulations was sufficient to preclude numerical emittance growth. A thin lens alternate gradient transport system with a phase advance of 90 degrees per magnet pair has been assumed for all the simulations reported here.

When a system of linear lenses is used to propagate a beam with a K-V distribution, the space charge forces are linear and oppose the net focusing forces. All the particles then execute orbits with the same phase advance per cell and that phase advance is reduced from the low current value. This reduced phase advance is a measure of the amount of current being transported. In fact, for a matched beam with a K-V distribution being transported in a thin lens alternate gradient transport system, only two parameters are required to completely specify the system. So, for example, specifying the phase advance in the absence of space charge and also the reduced or depressed phase advance completely specifies the system. Any other way of specifying the total current can also serve instead of the depressed tune as a second parameter.

For a K-V system being transported by finite lenses a measure of the transported current can be derived [12] by writing the envelope equations in normalized form. For a thin lens system, however, the appropriate [27] measure of beam intensity is:

$$Q = \frac{4 q^2 N r_p f}{A \beta \gamma^2 \epsilon} \quad (1)$$

where q and A are the ion charge state and mass number, N is the number of particles per unit length, r_p is the classical proton radius, $\pi \epsilon$ is the emittance, and f is the thin-lens focal length.

Several runs have been performed and these are summarized in Table I. The cases run are identified by the depressed tune, σ . Also tabulated are the values of Q as defined in Eq. 1. The last column in Table I is the number of filaments, M , formed in the phase space distribution by the unstable fields. Note that the first two cases are stable.

Figure 1 is a plot of 2048 sample particles (of the 16K in the run) showing four projections of the 4-dimensional $x-P_x-y-P_y$ phase space. This plot is of the initial matched K-V distribution of one of the runs. A K-V distribution which has the form

$$f(r,p) = \delta \left[\left(\frac{x}{x_o} \right)^2 + \left(\frac{y}{y_o} \right)^2 + \left(\frac{P_x}{P_{x_o}} \right)^2 + \left(\frac{P_y}{P_{y_o}} \right)^2 - R_o^2 \right] \quad (2)$$

has a uniform projection in each of the four views shown in Figure 1. The graininess of the plots is therefore due to the statistical variations in the sample.

Figure 2 is a similar plot of the phase space of the 45 degree case, but shown after the initial equilibrium has passed through 29 magnet pairs. Three well defined filaments can be seen in both the $x-P_x$ and $y-P_y$ projections. Phase space filamentation of this type, which can also be caused by lens non-linearities, is known [28] to cause emittance growth. This is also the case here. It is worth noting, however, the distinction between non-linearities due to external forces and those seen here. In the cases shown here, the non-linearities grow in proportion to their own amplitudes (exponential growth), at least in the early stages of the instabilities. Also since the theory of these instabilities, which examines small perturbations about an equilibrium, does not predict any emittance growth, it is expected that any emittance growth will only occur when the unstable perturbation is no longer small. For a particular mode therefore, the observation of filamentation and emittance growth is likely to occur near the point where the growth of that unstable mode is saturating.

Figure 3 is a plot of the rms emittances $x_{rms}P_{x_{rms}}$ and $y_{rms}P_{y_{rms}}$ (the cross terms in the normal definition [18] are negligibly small) as the beam evolves from its initial K-V equilibrium. These emittances initially remain constant as the unstable modes grow from their small initial values which are non-zero due to the statistical imperfections in approximating the initial distribution by a small number (in this case 16384) particles.

Once the initial perturbation has grown to a finite value, the beam phase space density rapidly filaments and the emittance grows until a saturated state is reached. The growth then stops. The rapid

growth of this mode is in agreement with the linear theory of the stability of K-V distributions in alternate gradient systems. Because only one unstable mode is present for a system with a depressed tune of 45 degrees, it has been possible to obtain detailed agreement with the theoretical predictions as to growth rate and eigenfunction characteristics for this case [5]. As pointed out previously this agreement occurs only before the major part of the emittance growth is observed.

When the initial current is increased the structure of the most visible unstable mode changes. Figure 4 shows the phase space after 20 magnet pairs of an initial K-V distribution with enough current to depress the phase advance from 90 degrees to 30 degrees. In this case, four filaments are visible. Figure 5 shows a continuation of this trend when the tune is depressed further to 15 degrees. Finally, Fig. 6 shows the case with tune depressed to 7.5 degrees. In this case the filaments are not quite as well defined but about 8 to 10 of them are present. The more current therefore, the greater the number of filaments which are visible. However, the mode which causes the most phase space structure, and is therefore the most visible, is not necessarily the only one that is unstable. In the higher current regime it is in fact likely that several modes are simultaneously unstable.

Figure 7 is a plot of the x and y rms emittances for the simulation of the case with a 30 degree depressed tune. The general behavior, i.e., a period of constancy followed by a period of rapid growth and then a steady state after saturation of this growth is similar to the 45 degree case. The growth rate in this case is faster. There is also an anisotropy in the emittance in the final state which appears to be due to the statistical excitation of the y-growing eigenfunction at a higher amplitude because of the particular set of random initial conditions on the particles.

Figure 8 illustrates the occurrence of a transition in behavior when the tune is depressed further. The emittance is again a constant initially and then grows rapidly. However, instead of reaching a steady state, the emittance continues to grow slowly. Since the distribution function by this time has evolved far from the initial K-V equilibrium, it is difficult to say whether this growth is caused by unstable modes which were unstable initially or modes which appeared as a result of the change in the distribution function, or in fact, whether the growth is caused by the non-linearities of the distribution which resulted after instability saturation. However to rule out numerical effects as a cause for this

emittance growth, several numerical tests were run in which quantities such as the number of particles and the spatial resolution of the numerical grid were changed. In none of these cases was the growth rate of the emittance affected substantially.

The simulation run with a depressed tune of 7.5 degrees, as shown in Fig. 9, exhibits an even more pronounced persistence to the emittance growth. In order to completely rule out the possibility that this emittance growth was caused by particle-particle collisions, this case was run using 64000 particles. In this case the emittance has grown by about a factor of 1.5 between the end of the rapid growth period and the end of the run. This greater emittance growth as the current increases seems to indicate the possibility that there is a maximum current which can be stably transported. However, the magnitude of this current depends on the details of the scaling of a beam transport system and will be discussed in the next section.

The rms emittance is the product of a configuration space and velocity space component, each of which can evolve separately. Figure 10 shows, for the case with 45 degree depressed tune, a plot of the x-extent of the beam at the center of an x focusing lens as the system evolves. Three curves labelled r , a , and m at the right margin correspond to the rms, absolute average and maximum (the position of the maximally displaced particle) measures of the size.

Figures 11-13 show the same graphs for the runs with depressed tunes of 30, 15, and 7.5 degrees respectively. Both the rms and absolute average beam sizes change little. Therefore little of the growth in the rms emittance shown in Figures 3, 7, 8 and 9 occurs due to growth in the configuration space component. In all cases the maximum particle, or edge of the distribution function, has moved to about twice its initial value. The beam size has not increased much for most of the particles, but some particles have been scattered out to twice the initial edge of the beam.

Figures 14-17 are the corresponding graphs of the evolution of the beam extent in P_x space, also taken at the center of an x-focusing lens. These curves also illustrate that most of the growth, especially at the highest currents, is due to growth in the velocity component of the emittance. The edge of

the beam has moved way out in velocity space. Since the same spreading has not occurred in configuration space, this is an indication of the highly non-linear space charge forces near the edge of the beam, with the non-linearity becoming more pronounced at the higher currents.

These curves all refer to the behavior at the center of the x -focusing lenses. This was done because this is where the beam is at its maximum in the x direction, and it is therefore appropriate to look at the beam growth at this point in order to determine the size channel which would be necessary to propagate the beam.

The self-consistent equilibria corresponding to a K-V distribution are not difficult to visualize. All projections of the beam are uniform ellipses. The non K-V steady states which the system has evolved to in these simulations are somewhat more complex. Figure 18 shows four views of the $x-P_x-y-P_y$ phase space from the simulation with an initial 30 degree depressed tune after the beam has propagated through 100 magnet pairs. Figures 19 and 20 are contour plots of the $x-P_x$ and $y-P_y$ phase spaces of Figure 18. Adjacent contours are separated by a factor of four in density. This run was chosen because it was the highest current at which a steady state was reached. The shapes of the $x-P_x$ and $y-P_y$ contours differ because the plot was done in the center of an x -focusing lens. A similar contour plot done at the center of the y -focusing lens shows the expected reversal of the two plots.

Another set of plots can be generated of the configuration space and velocity space contours. These are most conveniently taken half way between the x -focusing and y -focusing lenses. At this plane a matched equilibrium is symmetric in the x and y directions. Figures 21 and 22 show these plots for configuration and velocity space respectively for the same case run with a 30 degree depressed tune taken at the end of the simulation.

The squaring of these contour lines is just one indication as to the difficulty of analytic characterization of the high space charge equilibria. This squaring increases as the current is increased. Since the contours in phase space are not ellipses, it is also an indication that any definition of emittance in terms of the percentage of particles within an elliptical phase space contour may not be appropriate.

For completeness, it is also possible to plot various cross sections of these curves. Figure 23 is such a cross section of Figure 21. Figure 23 is a plot of $f(x)$, the number density as a function of x , at the $y = 0$ plane integrated over all velocities. Because this curve is generated at the symmetry plane, it is the same form as a curve of $f(y)$ at $x = 0$. Figure 24 is a similar plot of $f(P_y)$ at $P_x = 0$ integrated over all positions. These curves are typical. A reasonable approximation to them can be obtained as the sum of a distribution with a parabolic profile and a smaller one with a linearly decreasing tail [21]. The number of such curves which can be generated for all the cases run is large. Most of the information contained in these curves can be summarized by noting that as the current increases, the contours get squared as do the configuration space cross sections. The velocity space cross sections develop increasingly long tails. The information of the length of these tails however, can be pretty satisfactorily estimated from the curves of the evolution of velocity vs. time (Figs. 14-17), by comparing the maximum velocity particle to the rms velocities. However at the mid plane the velocity and configuration behavior look generally similar to Figs. 23 and 24.

III. CONCLUSIONS

Current intensity depends on the ratio of current to emittance. Therefore as the current increases, if the emittance increases correspondingly, then the depressed tune is unchanged. In fact, if the distribution function remains unchanged, the beam is then represented by the same solution to Maxwell's equations in the transverse direction. It is possible from purely dimensional arguments to show that any solution to Maxwell's equations in the transverse direction corresponds to a family of solutions at different currents. These currents can be related to the power propagating in a transport system by the relation

$$P = C \left(\frac{A}{z} \right)^{4/3} (B_q \epsilon)^{2/3} (B\gamma)^{7/3} (\gamma - 1) \quad (3)$$

where P is the power in watts, A and z are the mass number and charge state, B_q is the quadrupole pole tip field in Tesla, and $\pi \epsilon$ is the emittance in meter-radians. The coefficient C contains the information on the current intensity and the beam distribution function.

This formula was first suggested by Maschke and was derived by Courant [29] for a K-V distribution. A different treatment was derived by Reiser [30]. The derivation in terms of purely dimensional considerations is presented in the appendix.

It is possible to determine a value for the coefficient C in Eq. (3) corresponding to any solution to Maxwell's equations in general, and therefore specifically for the distributions corresponding to each of the simulations performed. However, the power transported is expressed in Eq. (3) in terms of the pole tip field. Therefore because the simulations were performed using thin lenses, and these are unphysical as they require singular pole tip strengths, some assumption must be made about the magnet fill in the transport system. From the extensive linear stability calculations [13-15], it is known that, at least in the linear stages of the instability, the behavior of the system is largely insensitive to magnet fill as long as the phase advance per cell is kept unchanged. This insensitivity to lens fill has also been seen in simulations [7].

Laslett has suggested [31] the definition of a beam figure of merit, $F = Q/(u_{max})^{2/3}$, based on the behavior of the scaled envelope equation [12]. The coefficient C in Eq. (3) is related to F by, $C = 3.43 \times 10^{15} F$ in MKSA units. For a K-V system, the values of F have been calculated for a range of parameters [31-33]. These results are plotted in Fig. 25, as a function of depressed tune, for a system with 90 degree phase advance and with 50 percent lens fill. The values of F can be calculated beyond the range shown in Fig. 25 from the expression [31] $F = 9.5 \sigma^{-2/3}$, which is accurate to within one percent below 10 degree depressed phase advance. From the K-V values, it is possible to calculate the value of F , and therefore the coefficient C , appropriate to the final state in each of the simulation runs.

Since the current does not change during the simulation, the coefficient in Eq. (4) changes due to the growth in emittance as the beam evolves. Because the beam size also increases an additional factor must be included to account for the fact that the magnet pole tip must be moved out. These values are listed in Table II. The value at 60 degrees, which is not unstable, is the same as Laslett's value. The other values are calculated from Laslett's values by dividing by the increase in rms emittance to the $2/3$ power and then also dividing by the increase in size to the beam edge (as measured from Fig. 13-16)

also raised to the 2/3 power. This second factor is necessary if the pole tip is moved out far enough to include the entire beam. Since the emittances used are rms emittance these particular coefficients are valid only when using this rms measure.

The last two entries in the table correspond to distributions which are not in steady state, but are still evolving. Notice for example that the initial figure of merit increases by a factor of 1.6 between 15 and 7.5 degrees, by the end of the run this improvement has been reduced to 1.2. If the run were continued further, this reduction would have continued still further resulting in the possibility of no gain in transported current intensity.

For the simulations performed, that is a constant current propagating down a uniform transport line, a K-V system can become rapidly unstable. This rapid instability appears to saturate after about a factor of two growth in emittance. At the highest current intensities studied, this period of rapid growth is followed by a period of slower growth which tends to limit the current intensity than can be propagated over long distances.

Because of the inherently non-linear nature of the phenomena involved it is difficult to say anything about beam distributions more general than K-V. If it is assumed that the behavior of non K-V distributions is adequately represented by the behavior of the simulations after initial saturation, then it would be possible to propagate very intense currents for modest distances without too much emittance growth. However the existence of modes which can grow rapidly and which could be excited if the beam distribution would evolve to a state closer to a K-V distribution, suggests that caution be exercised. Conservative design still seems to preclude operation in this space charge limited regime without a much fuller understanding of the effect of beam distribution function on stability.

ACKNOWLEDGMENTS

The author would like to thank Drs. L.J. Laslett, A.W. Maschke and L. Smith for their encouragement and assistance.

REFERENCES

1. T.F. Godlove and D.F. Sutter, "The U. S. Program in Heavy Ion Beam Fusion," paper CN-37-V-3 in *Plasma Physics and Controlled Nuclear Fusion Research 1978* (IAEA, Vienna, 1979).
2. Terry Godlove, "Review of Heavy Ion Fusion," *IEEE Trans. Nucl. Sci.*, NS26 (June 1979).
3. Robert L. Gluckstern, "Oscillation Modes in Two Dimensional Beams," in *Proceedings of the 1970 Proton Linear Accelerator Conference*, edited by M.R. Tracy (National Accelerator Laboratory, Batavia, Ill., 1970), Vol. 2, p. 811
4. M. Promé, "Effects de la Charge d'Espace dans les Accélérateurs Linéaires à Protons," thesis, Orsay, No. 7671 (1971).
5. L.J. Laslett and L. Smith, "Stability of Intense Transported Beams," *IEEE Trans. Nucl. Sci.*, Vol. NS26, p. 3080 (June 1979).
6. I. Hofmann, "Fluid and Vlasov Stability of Intense Ion Beams in Periodic Channels," *IEEE Trans. Nucl. Sci.*, Vol. NS26, p. 3083 (June 1979).
7. S. Penner and A. Galejs, "Transport Calculations for Very High Current Beams," *IEEE Trans. Nucl. Sci.*, Vol. NS26, p. 3086, (June 1979).
8. P.M. Lapostolle, "Etude Numerique d'Effets de Charge d'Espace en Focalisation Periodique," CERN-ISR/78-13 (CERN, Geneva, 1978).
9. G.W. Wheeler, K. Batchelor, R. Chasman, P. Grand and J. Sheehan, "The Brookhaven 200-MEV Proton Linear Accelerator," *Particle Accelerators*, Vol. 9, Nos. 1/2, Section II.2, p. 13, (Feb., 1979).
10. I.M. Kapchinskij and V.V. Vladimirkij, "Limitations of Proton Beam Current in a Strong Focusing Linear Accelerator Associated with Beam Space Charge," *Proc. Int. Conf. on High Energy Accelerators and Instrumentation*, edited by L. Kowarski, p. 274 (CERN, Geneva, 1959).

11. T.K. Kho and R.L. Martin, "Longitudinal and Transverse Space Charge Limitations on Transport of Maximum Power Beams," IEEE Trans. Nucl. Sci., Vol. NS26, p. 1025, (June 1977).
12. G. Lambertson, L.J. Laslett, L. Smith, "Transport of Intense Ion Beams," IEEE Trans. Nucl. Sci., Vol. NS26, p. 993, (June 1977).
13. Lloyd Smith, "Stability of the K-V Distribution in Long Periodic Transport Systems, Part I, General Formulation," LBL Report HIFAN-13, (Lawrence Berkeley Lab., Oct. 1977).
14. Swatan Chattopadhyay, "Stability of the K-V Distribution in Long Periodic Transport Systems, Part II, Equations Used for Numerical Computations," LBL report HIFAN-14, (Lawrence Berkeley Lab., Oct. 1977).
15. Ingo Hofmann and L. Jackson Laslett, "Stability of the K-V Distribution in Long Periodic Transport Systems, Part III, Computational Results," LBL report HIFAN-15, (Lawrence Berkeley Lab., Oct. 1977).
16. J. Bisognano, L.J. Laslett and Lloyd Smith, "Computational Study of a Third-Order Instability Suggested by Simulation Computations of Dr. Haber," LBL report HIFAN-43, (Lawrence Berkeley Lab., Sept. 1978).
17. J. Bisognano, L.J. Laslett and Lloyd Smith, "Third-Order-Mode Performance for an Interrupted Solenoid Transport System," LBL report HIFAN-44, (Lawrence Berkeley Lab., Sept. 1978).
18. P.M. Lapostolle, "Possible Emittance Increase Through Filamentation Due to Space Charge in Continuous Beams," IEEE Trans. Nucl. Sci., Vol. NS18, p. 1101, (1971).
19. Frank J. Sacherer, "RMS Envelope Equations with Space Charge," IEEE Trans. Nucl. Sci., Vol. NS18, p. 1105, (1971).

20. Ingo Hofmann, "Influence of the Distribution Function on Eigenoscillations and Stability of a Beam," LBL Report HIFAN-79, (Lawrence Berkely Lab., Dec. 1978), submitted for publication to *Phys. Fluids*.
21. I. Haber, "Space Charge Limited Transport and Bunching of Non K-V Beams," *IEEE Trans. Nucl. Sci.*, Vol. NS26, p.3090 (June 1979).
22. I. Haber, "Space Charge Limited Transport and Bunching of Non K-V Beams," *NRL Memorandum Report 4050*, (Naval Research Lab., Washington, D. C., July, 1979).
23. I. Haber and A. W. Maschke, "Steady State Transport of High Current Beams in a Focused Channel," *Phys. Rev. Letters*, Vol. 42, #22, p. 1479 (May 28,1979).
24. J.H. Orens, J.P. Boris, and I. Haber, "Optimization Techniques for Particle Codes," in *Proceedings of the Fourth Conference on Numerical Simulation of Plasmas*, Naval Research Laboratory, Washington, D. C., 1979, edited by J.P. Boris and R.A. Shanny, (Superintendent of Documents, Washington, D. C., 1971).
25. Irving Haber, "Computer Simulation of Space Charge Effects in Particle Accelerators," *NRL Memorandum Report 3705*, (Naval Research Lab., Washington, D. C., Jan. 1978).
26. I. Haber, "Collisional Emittance Growth in the Particle Simulation of Focused Beam Transport," *NRL Memorandum Report 3817*, (Naval Research Lab., Washington, D. C., July 1978).
27. Lloyd Smith, private communication.
28. J.D. Lawson, p. 197 in *The Physics of Charged Particle Beams* (Clarendon Press, Oxford, 1977).
29. E.D. Courant, "Power Transport in Quadrupole or Solenoidal Focusing Systems," *ERDA Summer Study of Heavy Ions for Inertial Fusion*, LBL-5543, p. 72, (Lawrence Berkeley Lab., December 1976).

30. M. Reiser, "Periodic Focusing of Intense Beams," *Particle Accelerators*, Vol. 8, p. 167, (1978).
31. L. Jackson Laslett, "The Figure of Merit, $q/\mu_{\max}^{2/3}$, for Beam Transport Through Periodic Focusing Systems," *Proceedings of the Heavy Ion Fusion Workshop*, BNL 50769, p. 112 (Brookhaven National Laboratory, 1978).
32. Victor O. Brady and L. Jackson Laslett, "The Figure of Merit," $Q'/u_m^{2/3}$, for Beam Transport Through a Periodic Quadrupole Lens System," LBL report HIFAN-11, (Lawrence Berkeley Lab., Sept. 1977).
33. L. Jackson Laslett, private communication.

Table I. Summary of Cases Run

σ	Q	M
90	0.0	—
60	0.93	—
45	1.6	3
30	3.1	4
15	6.2	6
7.5	12.4	8-10

Table II. Transport Figures of Merit Modified
by Space Charge Driven Instabilities

σ	F_n	F_{100}
60°	0.34	0.34
45°	0.56	0.22
30°	0.87	0.31
15°	1.52	0.54
7.5°	2.48	0.67

Appendix

CURRENT SCALING IN A STRONG FOCUSING CHANNEL

Consider a beam of charged particles, in the paraxial approximation, in a reference frame moving with the beam. The transverse dynamics, in this frame, is described by the Vlasov-Poisson system of equations.

$$\frac{\partial f}{\partial t} + \mathbf{v} \cdot \nabla f + \frac{q}{m} (\mathbf{E}_{ex} + \mathbf{E}) \cdot \nabla_{\mathbf{v}} f = 0 \quad (A1)$$

where the distribution function is normalized so that

$$\int f \, dv_x \, dv_y \, dx \, dy = 1,$$

and \mathbf{E}_{ex} represents the focusing magnet force in the beam reference frame. The space charge fields are found from

$$\nabla \cdot \mathbf{E} = 4\pi\rho. \quad (A2)$$

In order to investigate the scaling of this system we write these equations in terms of normalized variables. Setting $\mathbf{r} = r_0 \hat{\mathbf{r}}$, $\mathbf{v} = v_0 \hat{\mathbf{v}}$ and $t = t_0 \hat{t}$ with $r_0 = v_0 t_0$, and also $\mathbf{E}_{ex} = E_0 \hat{\mathbf{E}}_{ext}$

$$\frac{\partial f}{\partial \hat{t}} + \hat{\mathbf{v}} \cdot \hat{\nabla} f + \frac{r_0 q}{v_0^2 m} (E_0 \hat{\mathbf{E}}_{ext} + \mathbf{E}) \cdot \hat{\nabla}_{\hat{\mathbf{v}}} f = 0. \quad (A3)$$

Since the divergence operator is just a linear operator for the purpose of this scaling analyses, it can be formally inverted and written as:

$$\mathbf{E} = 4\pi L \rho \quad (A4)$$

where L is just the appropriate linear operator inverse to the divergence. The self-consistent electric field can then be written in terms of the total current I as

$$\mathbf{E} = \frac{4\pi I r_0 \hat{L}}{r_0^2 \beta \gamma c} \int f \, dv_x \, dv_y. \quad (A5)$$

Equation (A3) may then be rewritten as:

$$\frac{\partial f}{\partial t} + \hat{v} \cdot \hat{\nabla}_v f + (C_1 \hat{E}_{ext} + C_2 \hat{L} \int f dv_x dv_y) \cdot \hat{\nabla}_v f = 0$$

where

$$C_1 = \frac{r_0 q}{v_0^2 m} E_o \quad (A6)$$

$$C_2 = \frac{4\pi I q}{\beta \gamma c v_0^2 m}. \quad (A7)$$

Any distribution function f satisfy (A6) with a particular form of \hat{E}_{ext} will therefore be a solution for any combination of parameters which leave C_1 and C_2 unchanged. We can use this to derive a scaling relation for I .

Introducing an emittance

$$\epsilon = C_3 r_0 v_0 / \beta \gamma c, \quad (A9)$$

then

$$C_1 = \frac{q \epsilon \beta \gamma c}{m C_3 v_0^3 m}. \quad (A10)$$

Solving for the current

$$I = \left[\frac{C_2 c^{2/3}}{C_3^{2/3} 4\pi} \right] \left[\frac{m}{q} \right]^{1/3} \epsilon^{2/3} E_o^{2/3} \beta^{5/3} \gamma^{5/3}. \quad (A11)$$

If the external focusing force is written in terms of transverse magnetic fields, $E_o = \beta \gamma B_o$, this becomes

$$I = C_3 \left[\frac{m}{q} \right]^{1/3} \epsilon^{2/3} B_o^{2/3} (\beta \gamma)^{7/3}. \quad (A12)$$

The power transported by this current, is

$$P = (\gamma - 1) \frac{mc^2}{q} I$$

or

$$P = C \left[\frac{m}{q} \right]^{4/3} \epsilon^{2/3} B_o^{2/3} (\beta \gamma)^{7/3} (\gamma - 1) \quad (A13)$$

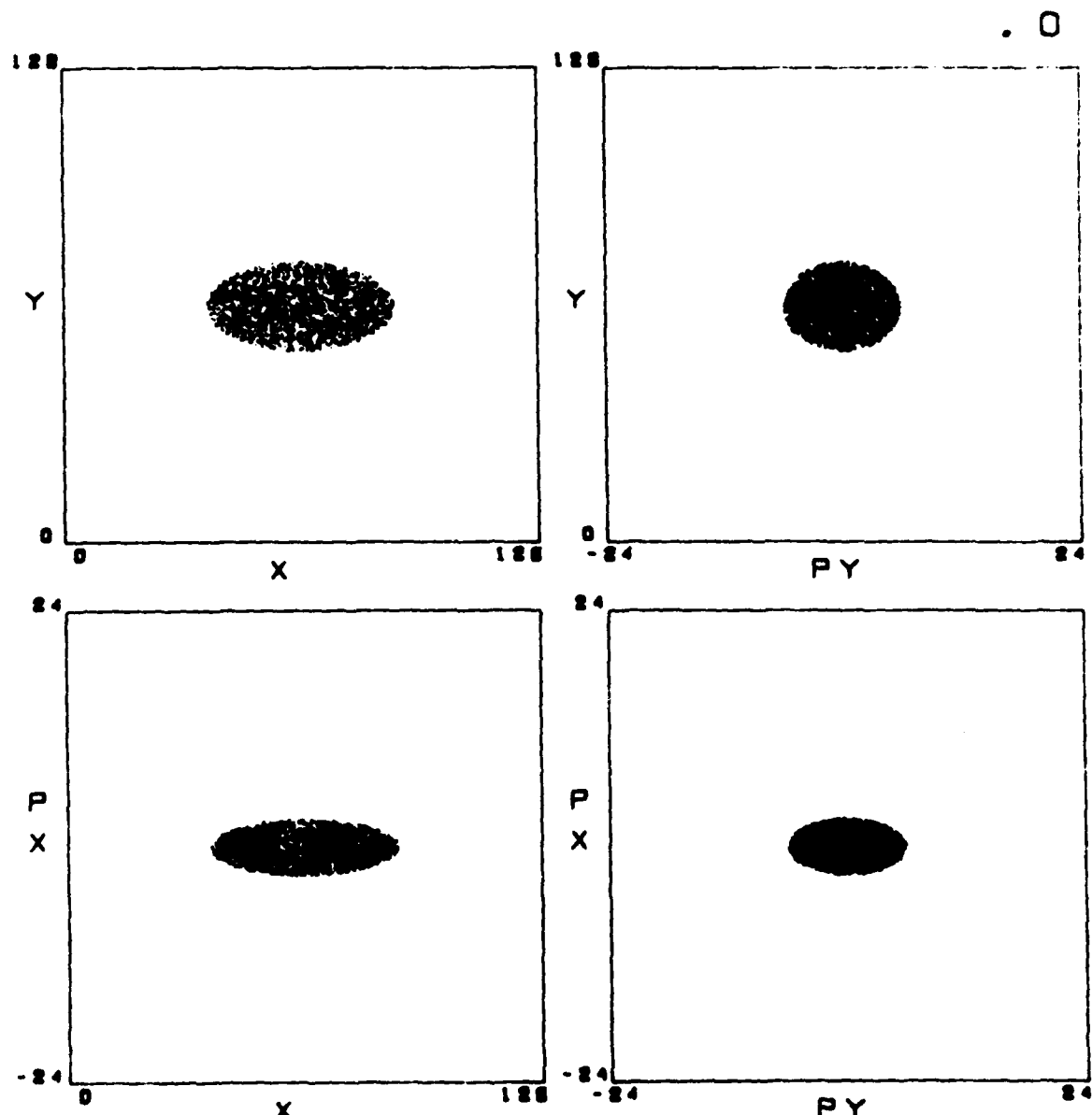


Fig. 1 — Four projections of the four-dimensional K-V distribution showing 2048 sample particles. The configuration space units are numerical grid cell and the velocity (momentum) units are in grid cells traversed in one magnet period.

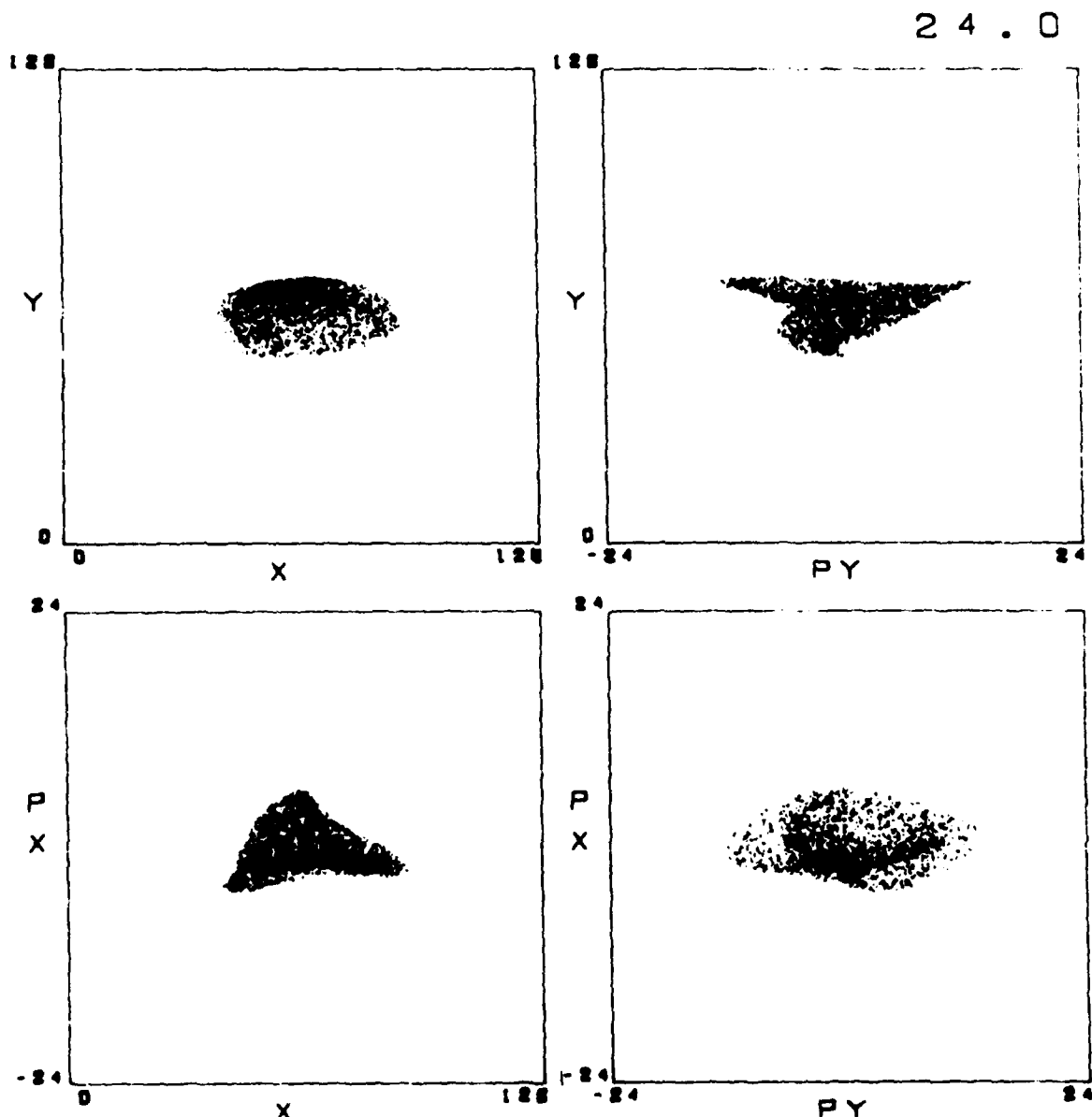


Fig. 2 - Four phase space projections showing filament formation in phase space after traversing 29 magnet pairs. The initial distribution is a K-V system with a depressed phase advance of 45 degrees.

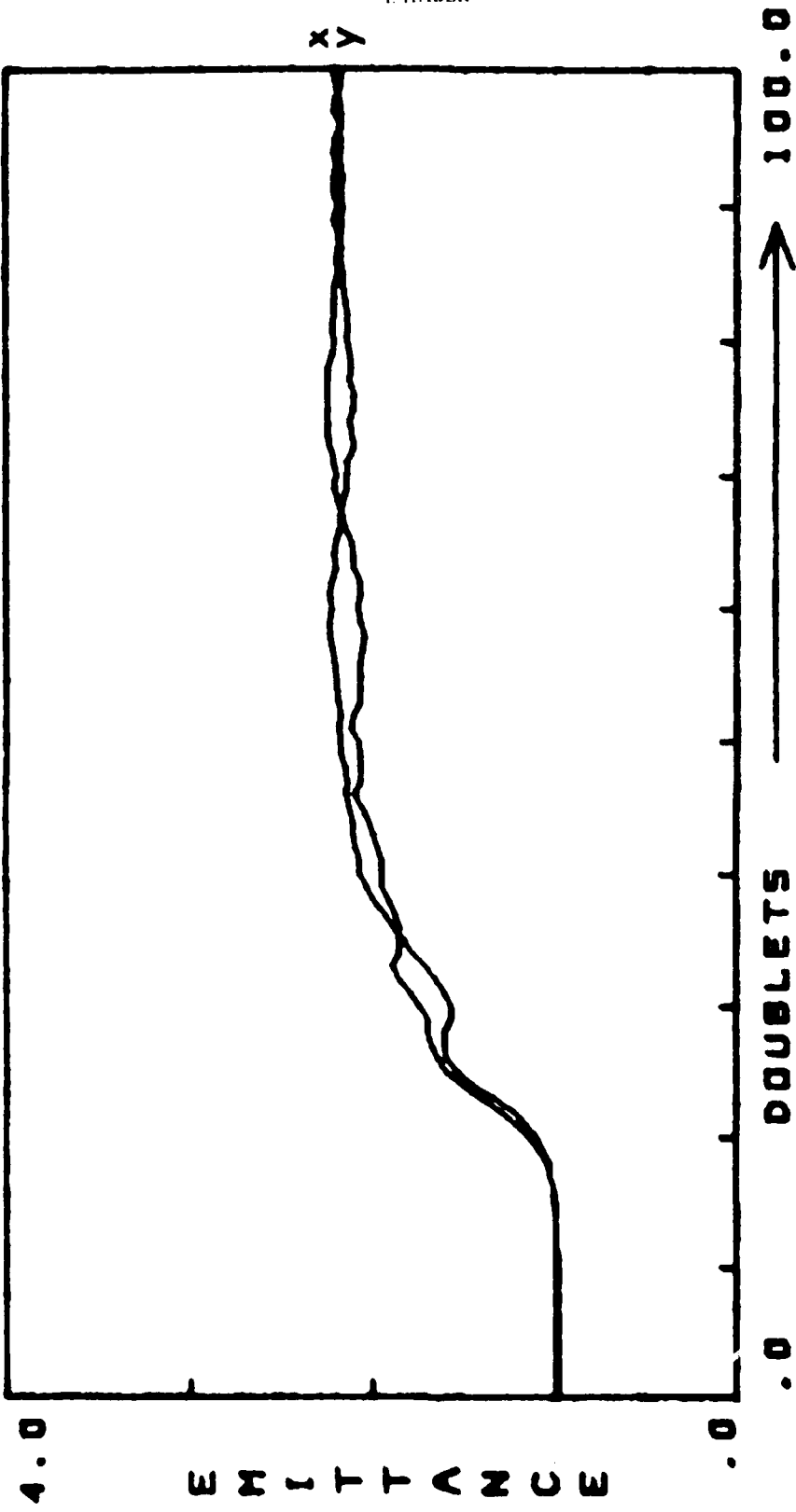


Fig. 3 - Evolution of the x and y rms emittances in a system with an initial matched K-V distribution with enough current to depress the tune from 90 degrees to 45 degrees. The vertical scale is normalized to the initial emittance. The horizontal scale is measured in alternate gradient magnet pairs.

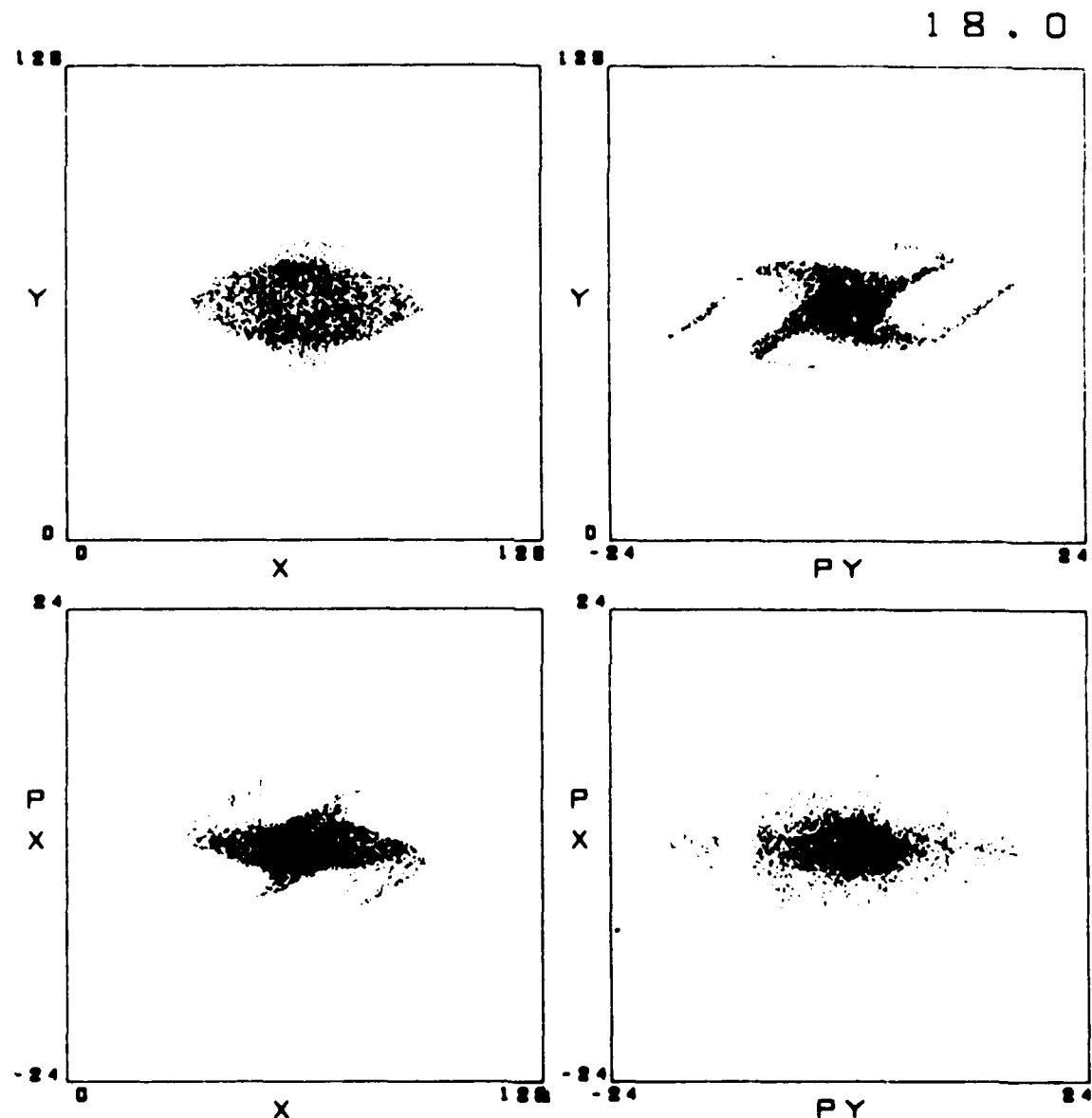


Fig. 4 — Four phase space projections showing the evolution, after 20 magnet pairs, of a K-V system with a depressed phase advance of 30 degrees

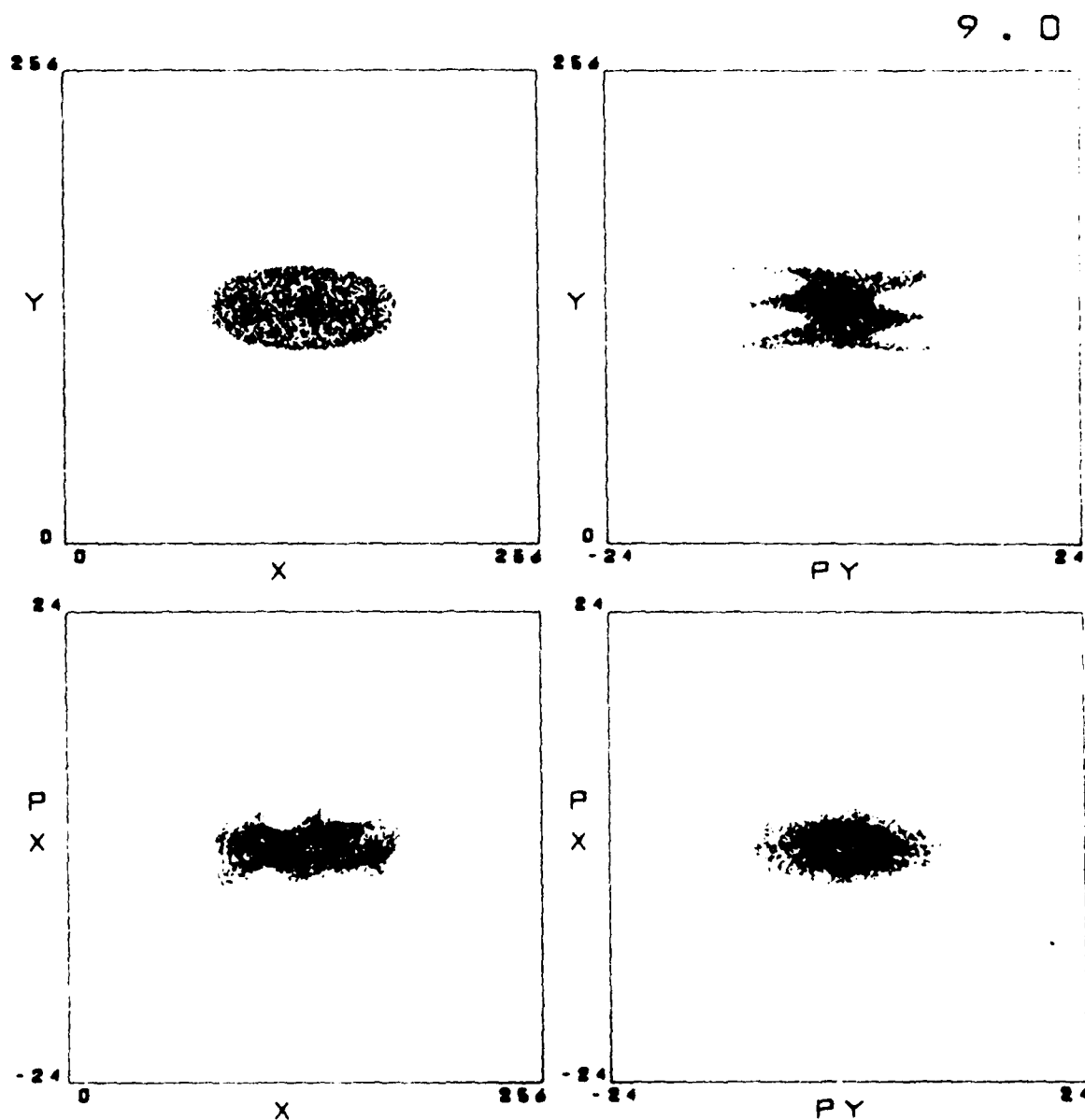


Fig. 5 - Four phase space projections, after 9 magnet pairs, of a system with a depressed phase advance of 15 degrees

1 3 . 0

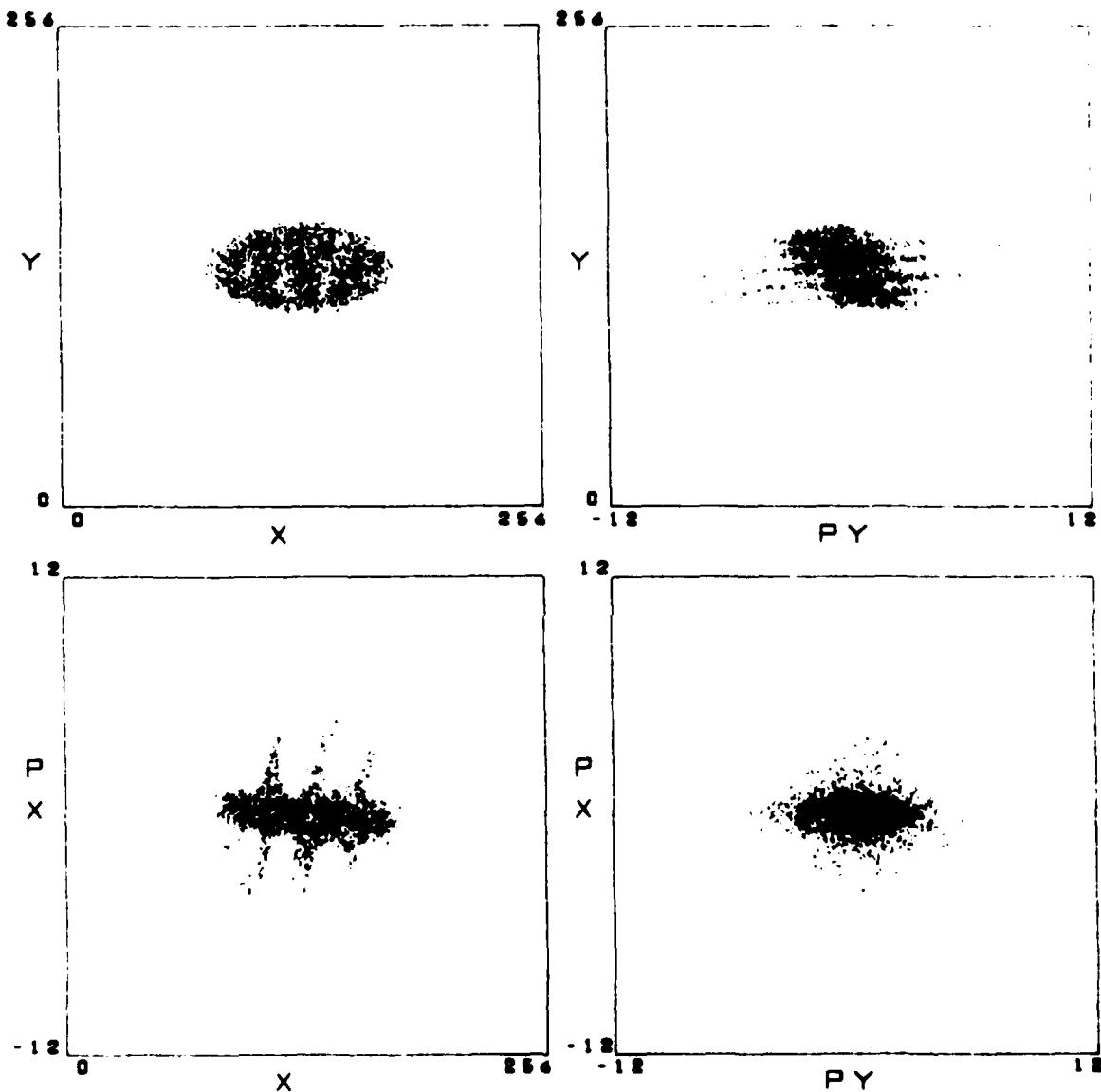


Fig. 6 - Four phase space projections, after 13 magnet pairs, of a system with a depressed tune of 7.5 degrees

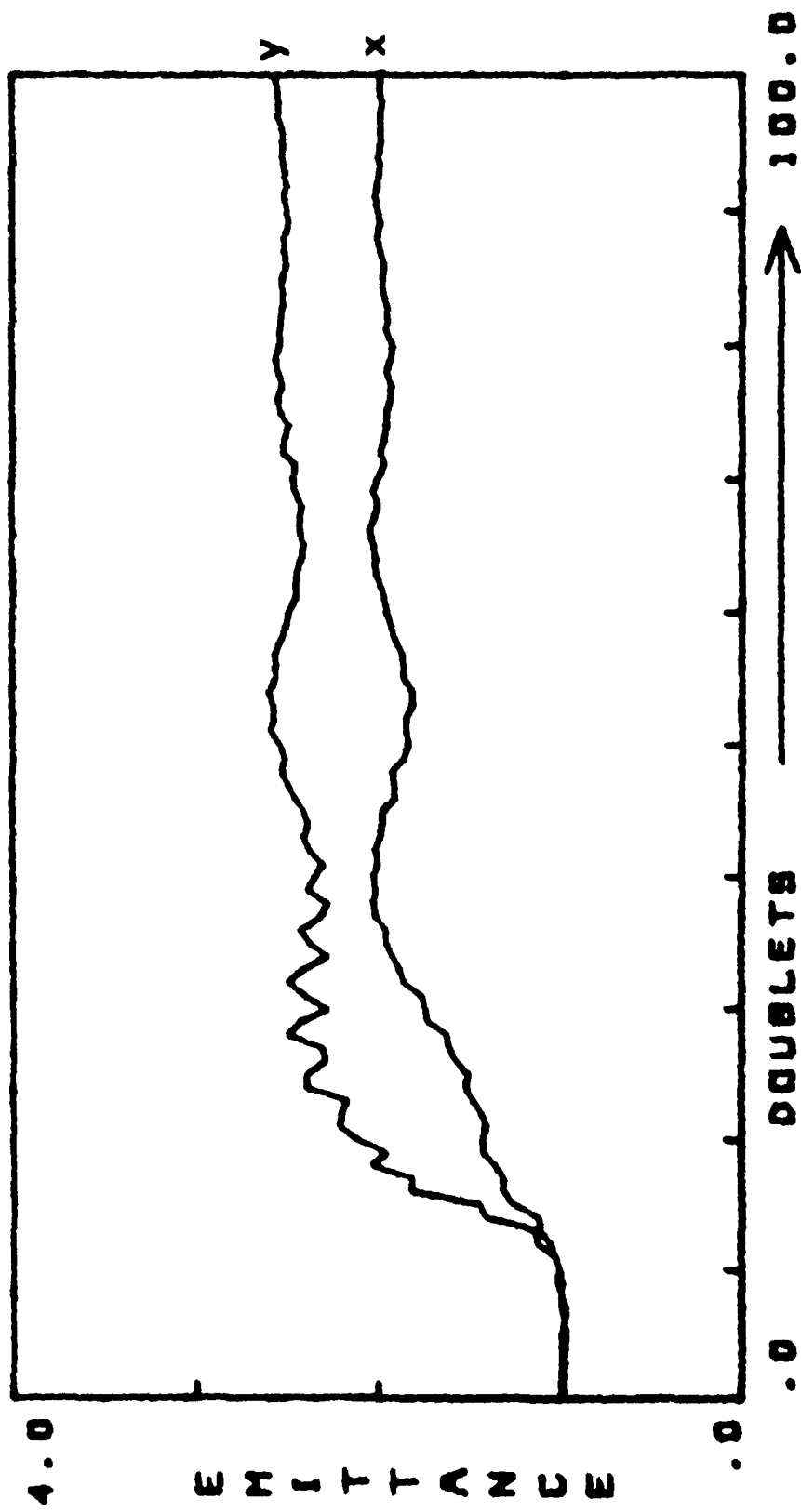


Fig. 7 - Evolution of the x and y rms emittances in a system with an initial K-V distribution with a depressed phase advance of 30 degrees

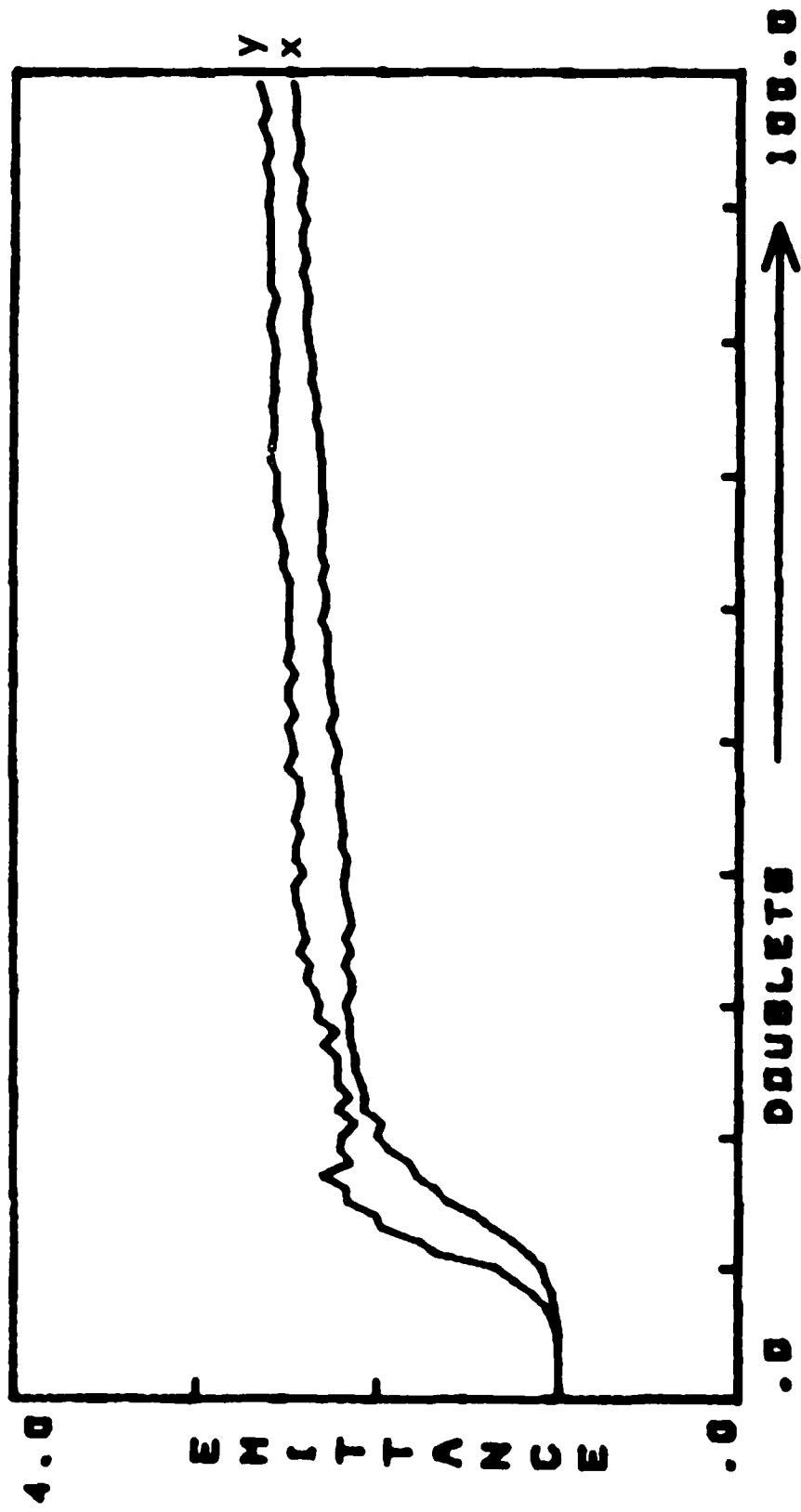


Fig. 8 - Evolution of the x and y rms emittances in a system with an initial depressed phase advance of 15 degrees.
Some slow long time scale growth in the emittance is apparent.

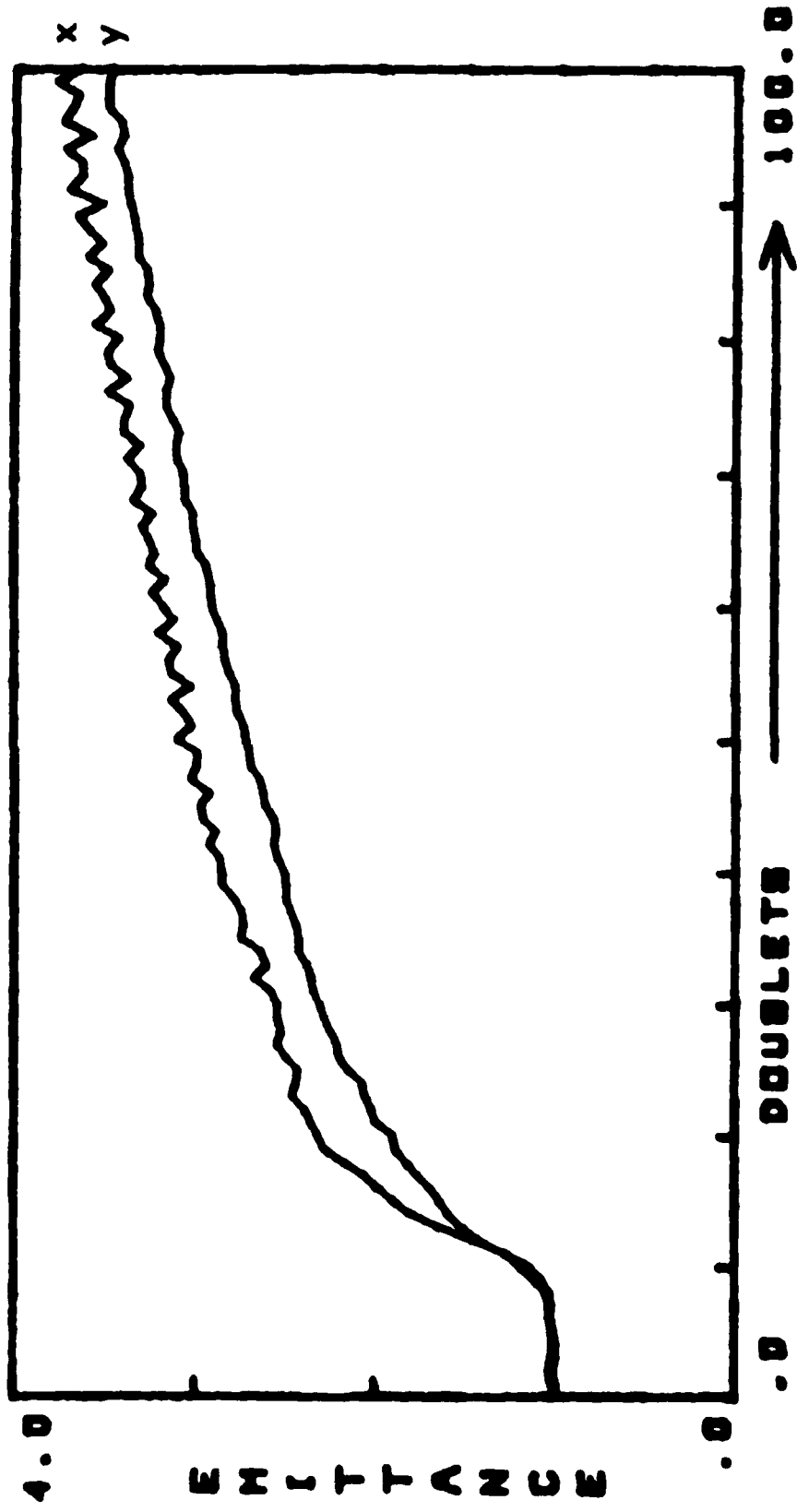


Fig. 9 Evolution of the x and y rms emittances in a system with an initial depressed phases advance of 7.5 degrees. The long time scale emittance growth is more pronounced than in the previous figure.

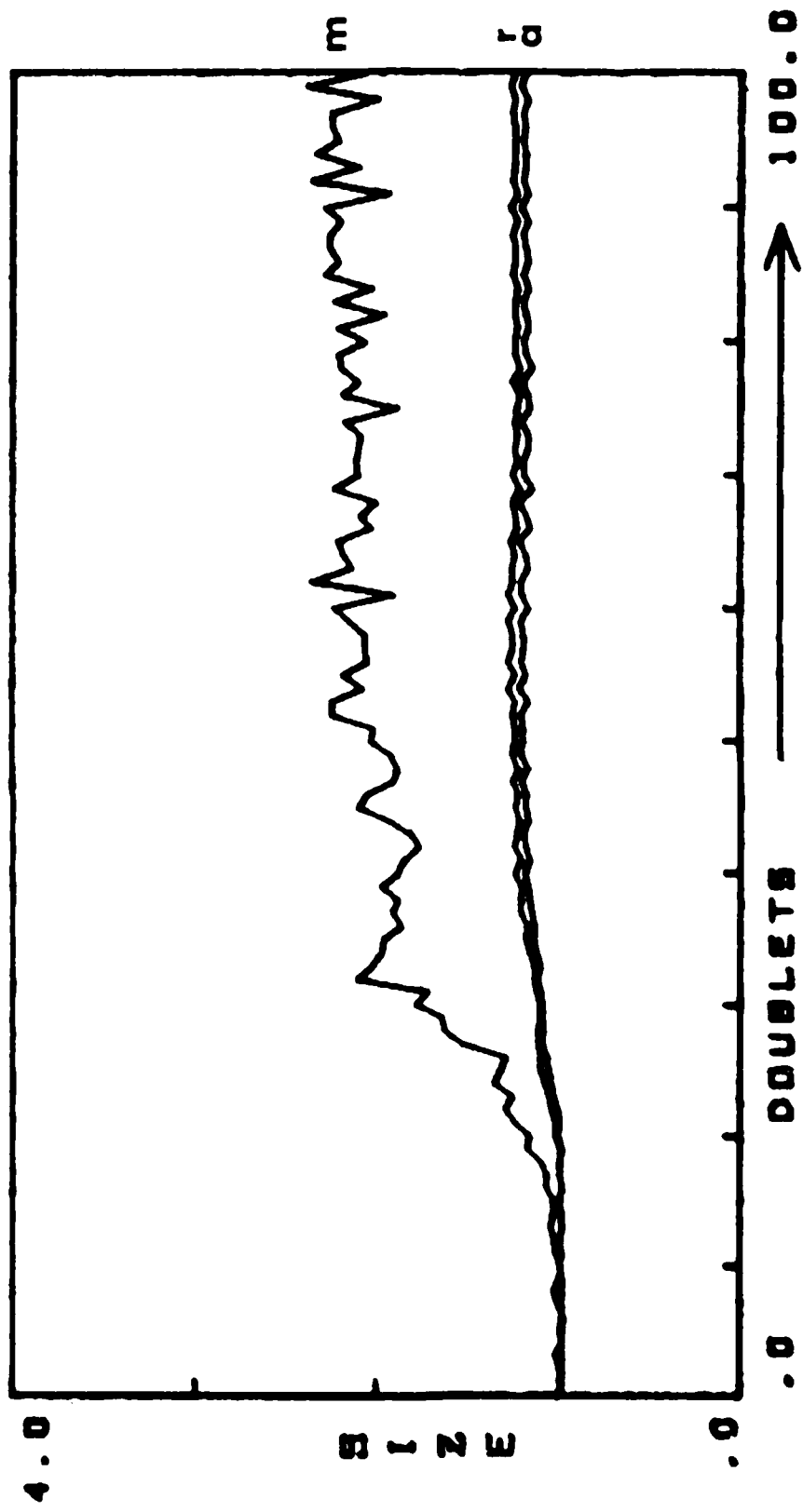


Fig. 10 - Evolution, for 45 degree depressed phase advance of the beam size, in the v direction, at the center of an focusing lens. The curves labelled r , a , and m correspond to size (normalized to the initial size) measured as rms, absolute average and location of the particle with the maximum value respectively.

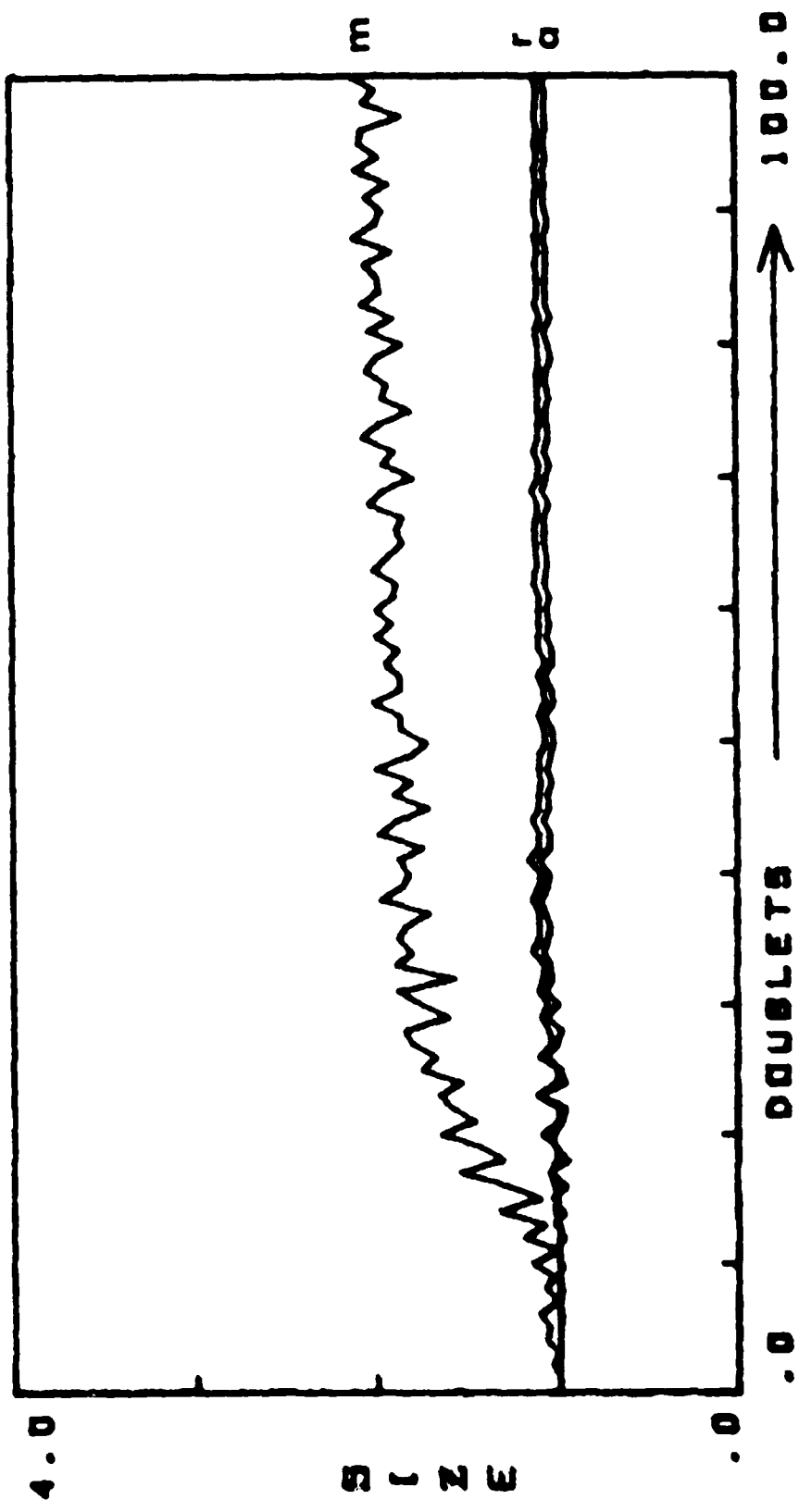


Fig. 1. Evolution of the beam size in the v direction for an initial 30 degree phase advance

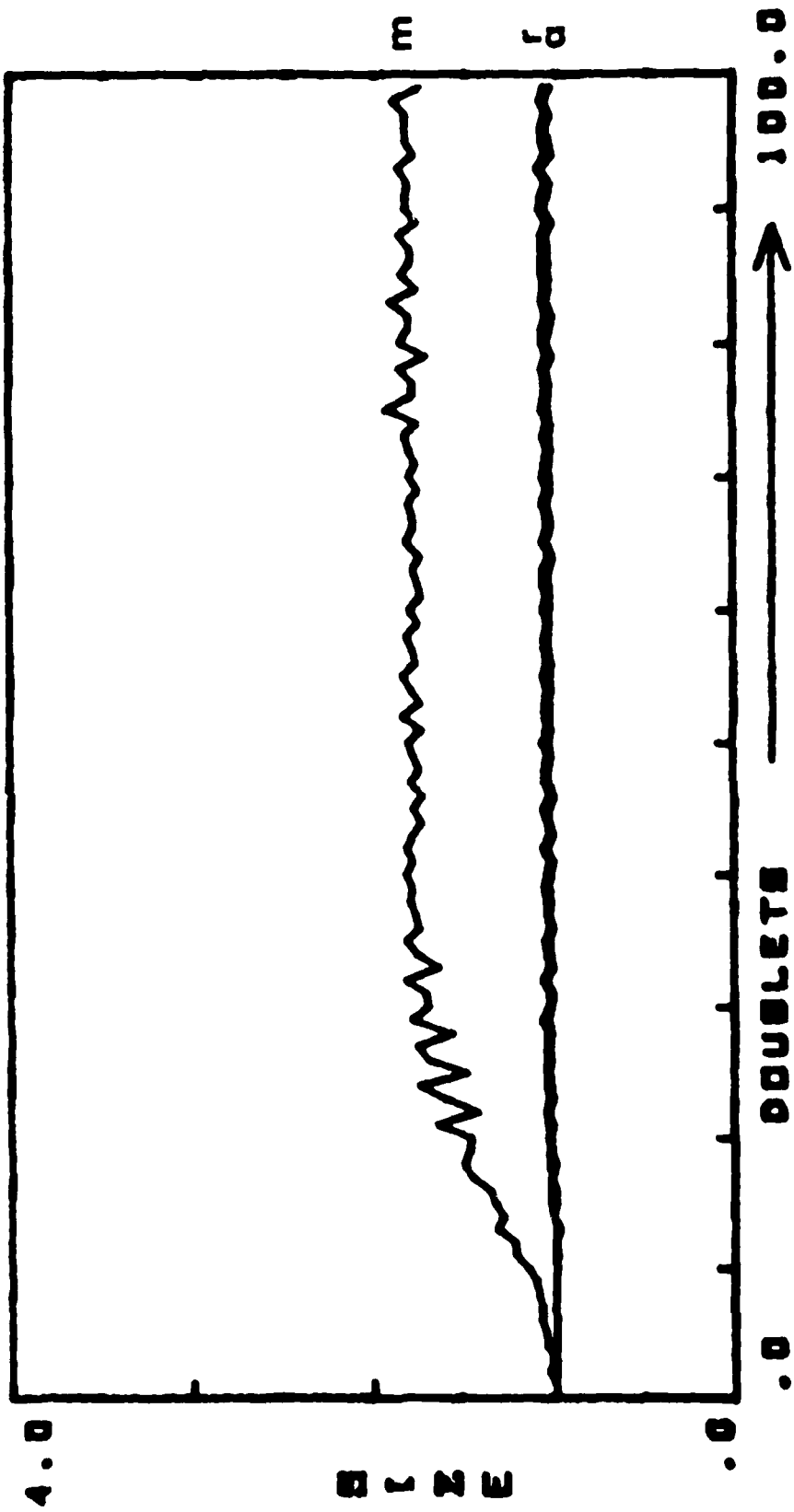


Fig. 12 - Evolution of the beam size in the x direction for an initial 15 degree phase advance

I. HABER

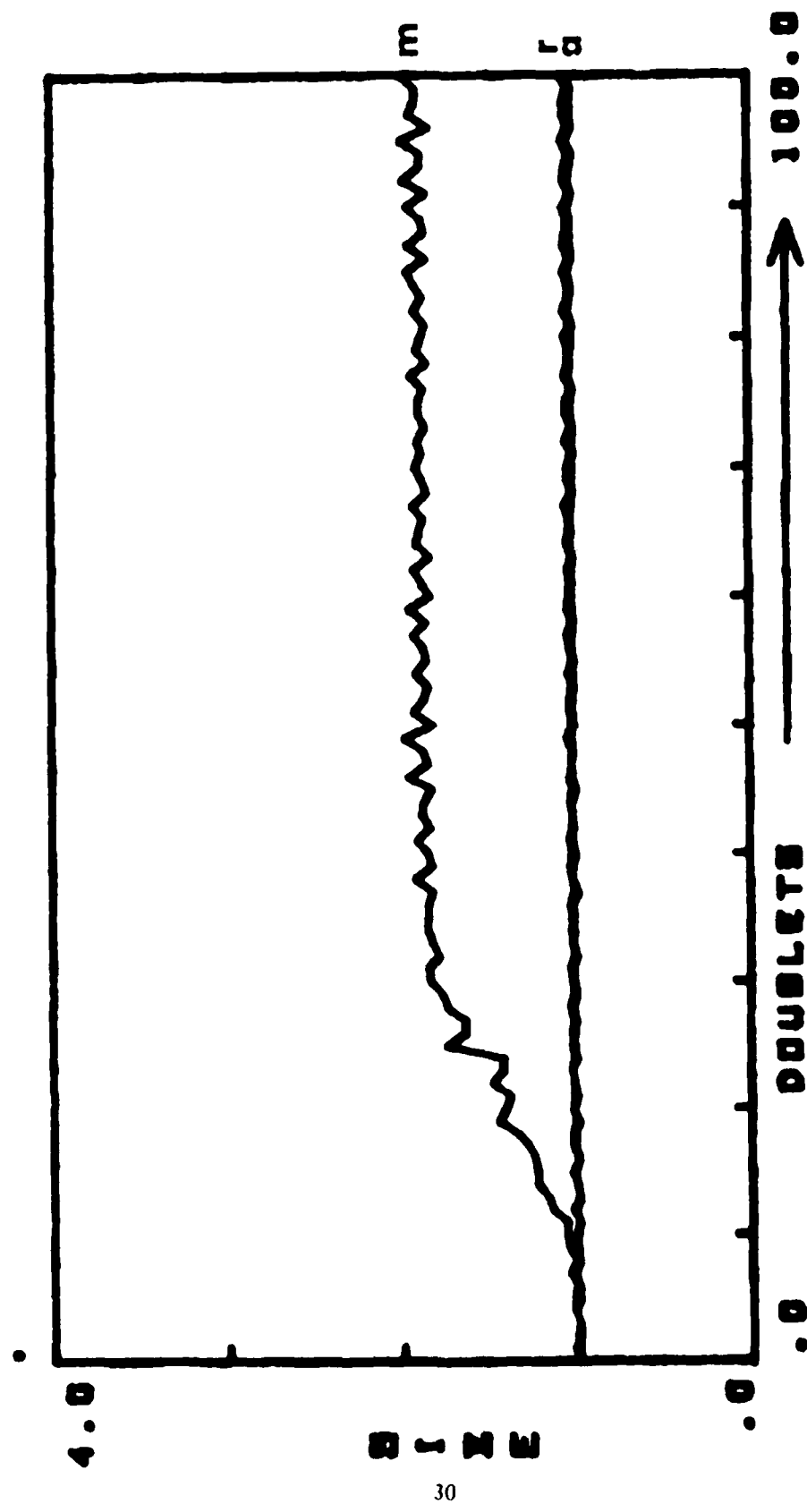


Fig. 11: - Evolution of the beam size in the x direction for an initial 7.5 degree phase advance

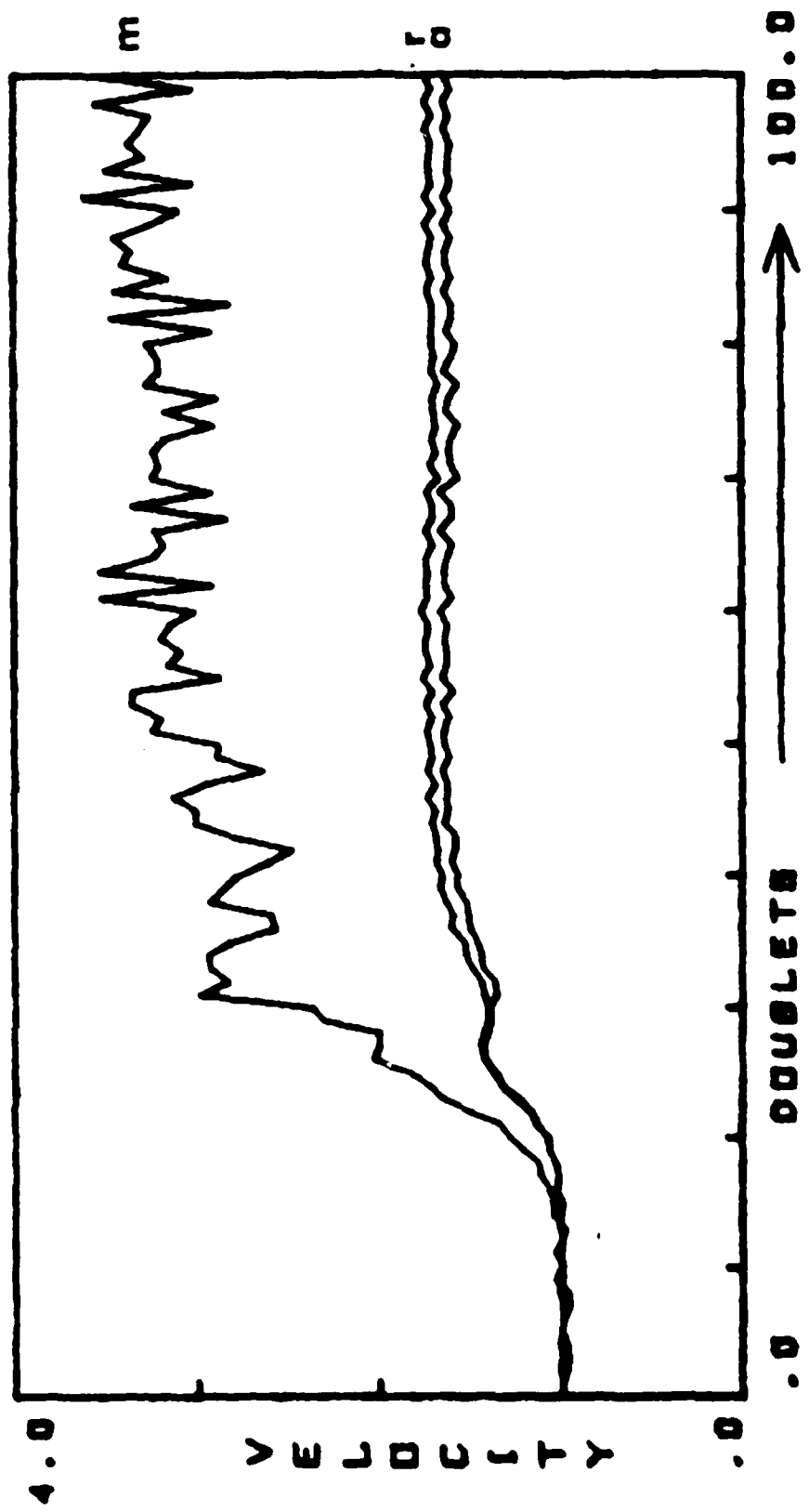
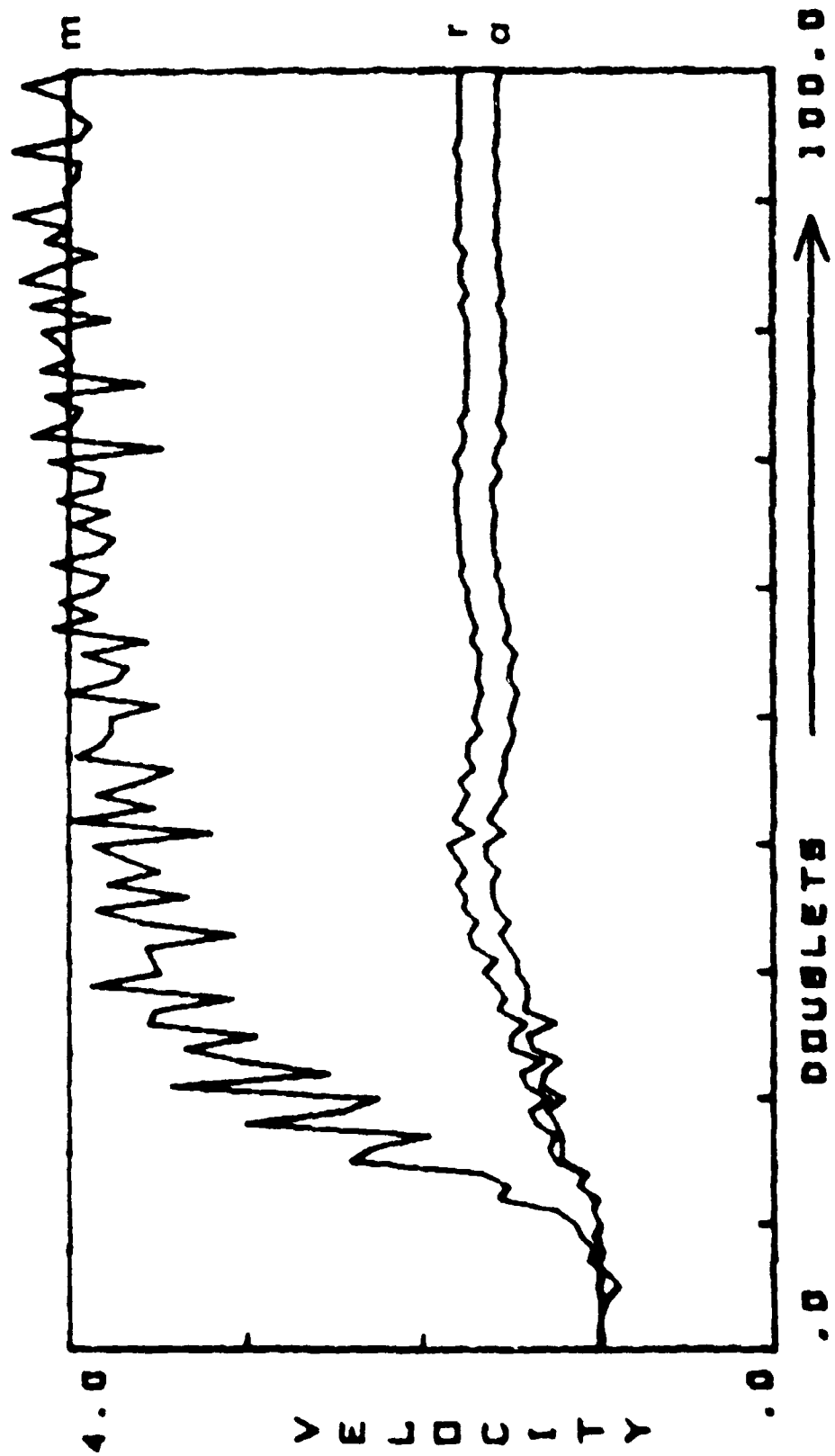


Fig. 14. Evolution of the rms, absolute average and maximum momenta at the center of an x-focusing lens, for the simulation with a 45 degree initial phase advance



Evolution of the v-momenta for the case with 30 degree initial phase advance

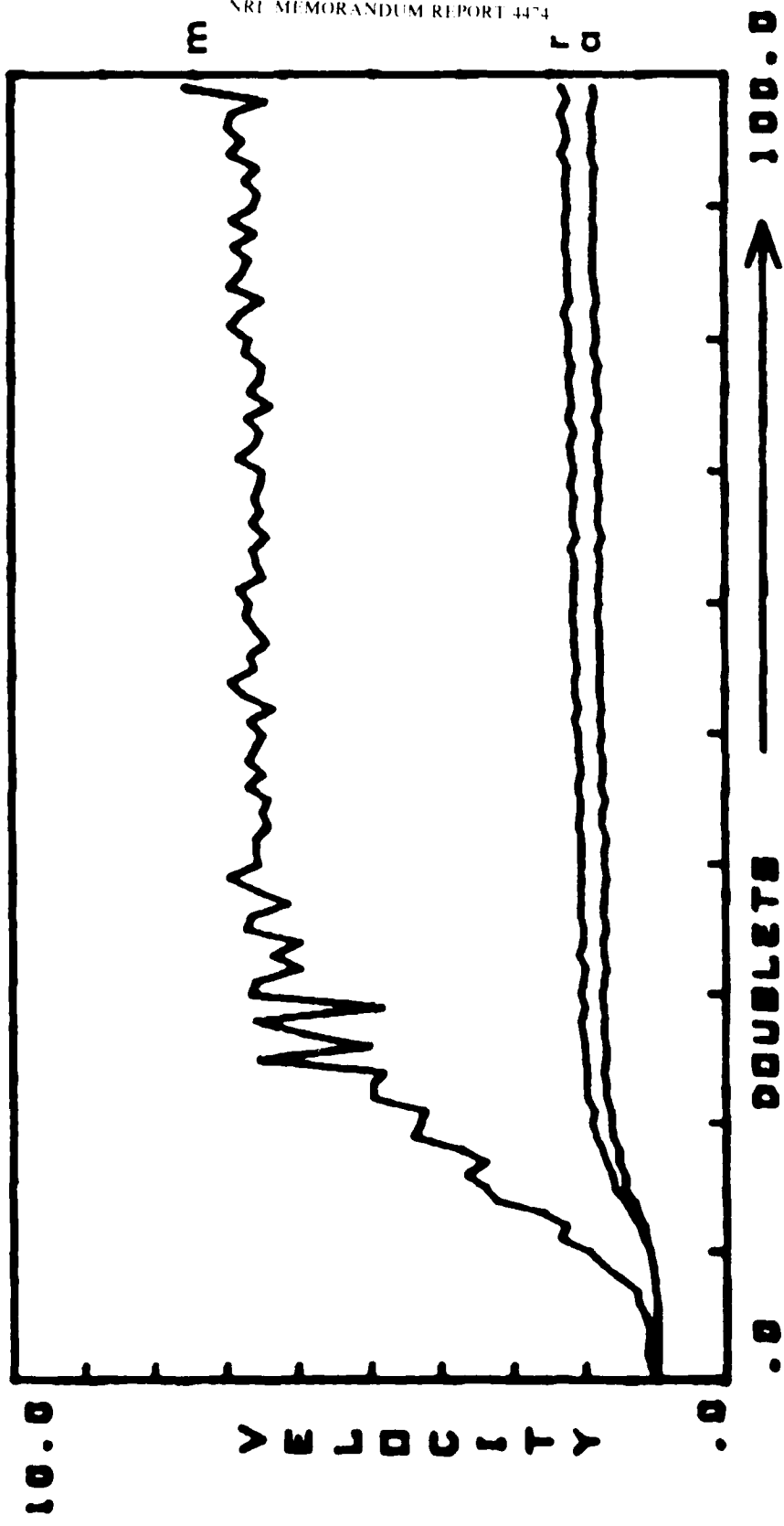


Fig. 1. Evolution of the v-momenta for the case with 15 degree initial phase advance

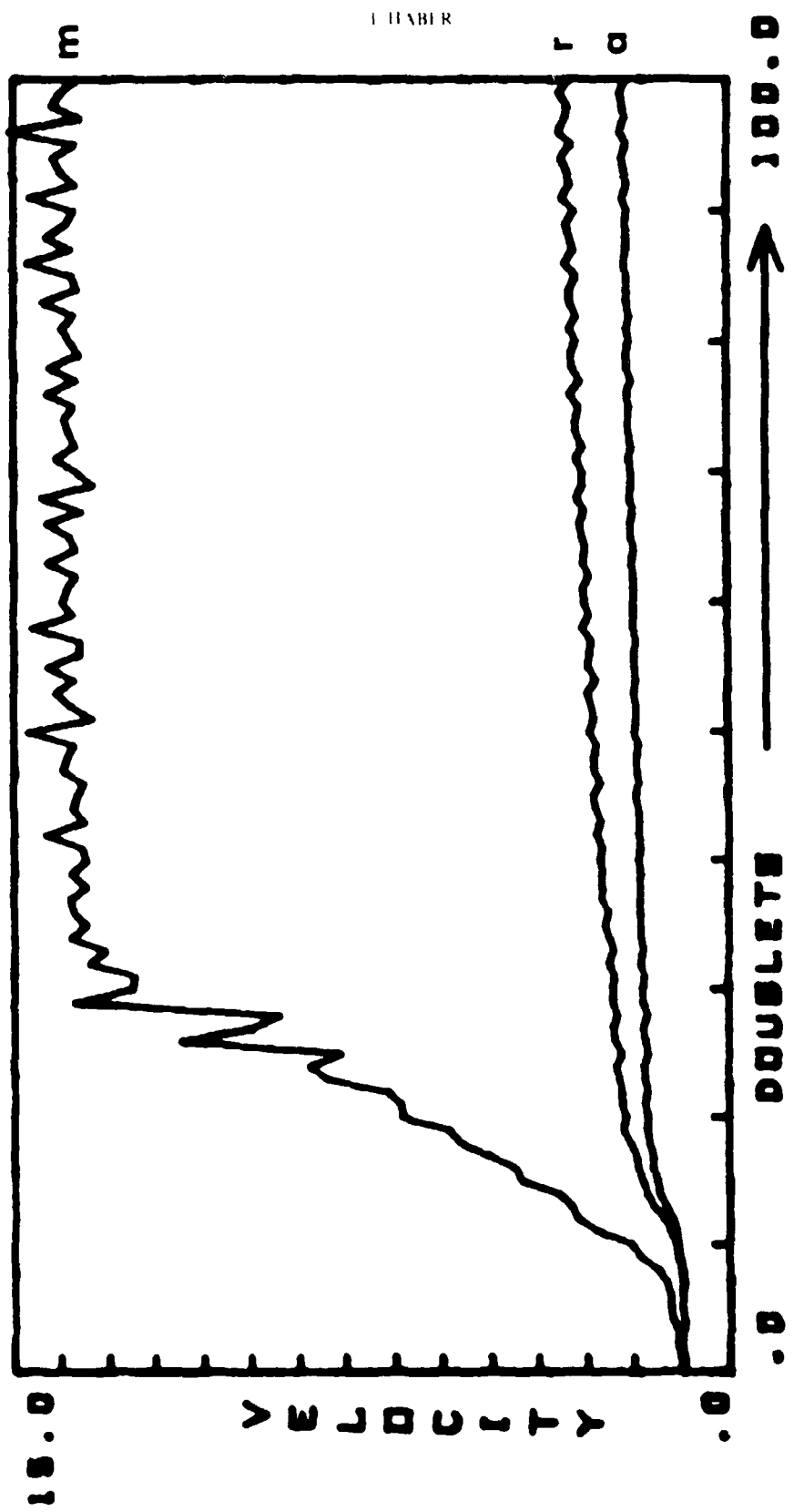


Fig. 11. Evolution of the x-momenta for the case with 7.5 degree phase advance.

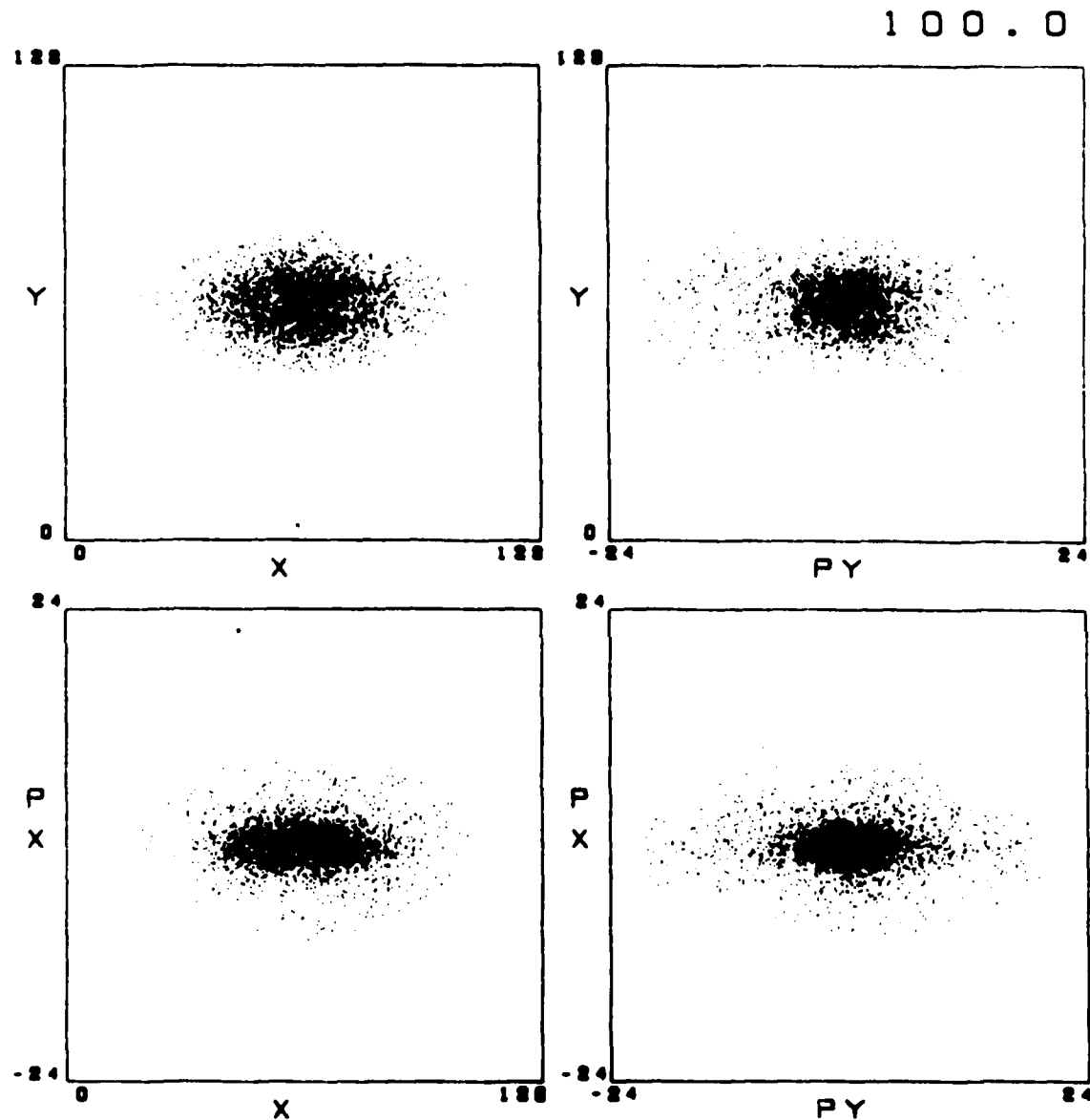


Fig. 18 -- Four views of the $x-P_x-y-P_y$ phase space of a simulation with an initial depressed phase advance of 30 degrees which has been propagated through 100 magnet pairs. The system has gone unstable and by this point has reached a steady state.

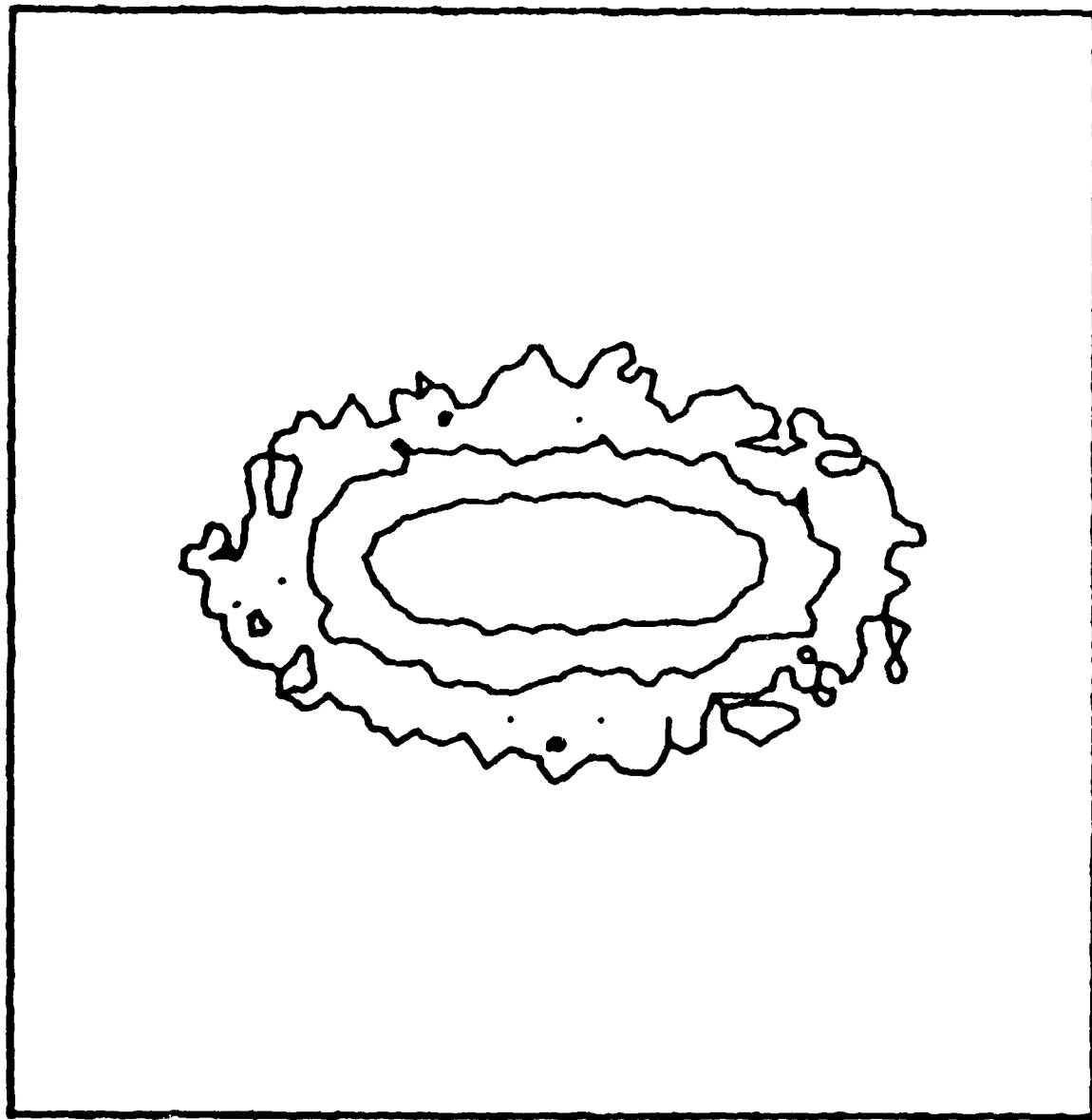


Fig. 19. — A contour plot of the $v - P_v$ phase space projection shown in Fig. 18. Adjacent contours are separated by a factor of four in density.

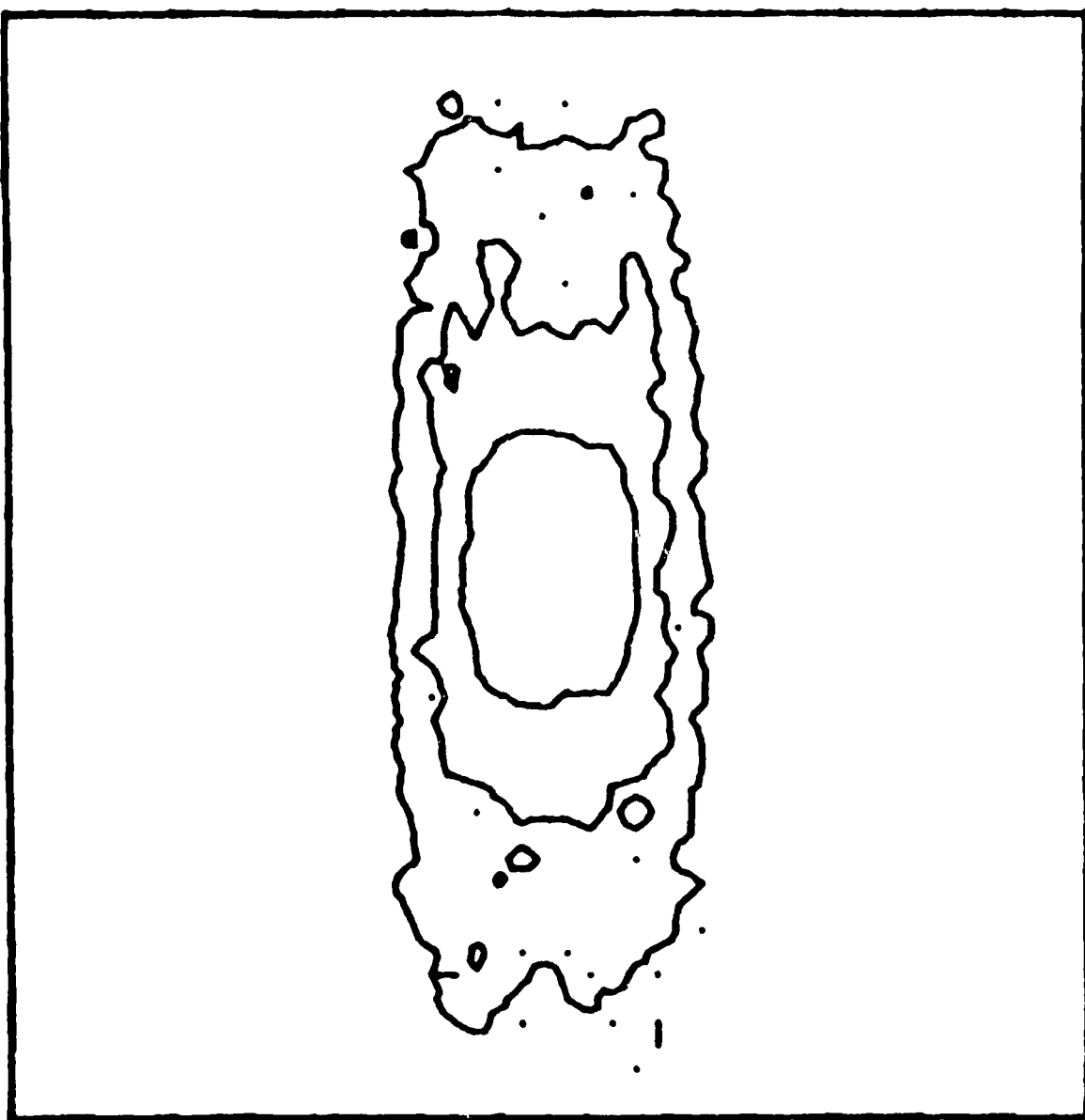


Fig. 20 - A contour plot of the $v - P$ phase space projection of Figure 18.

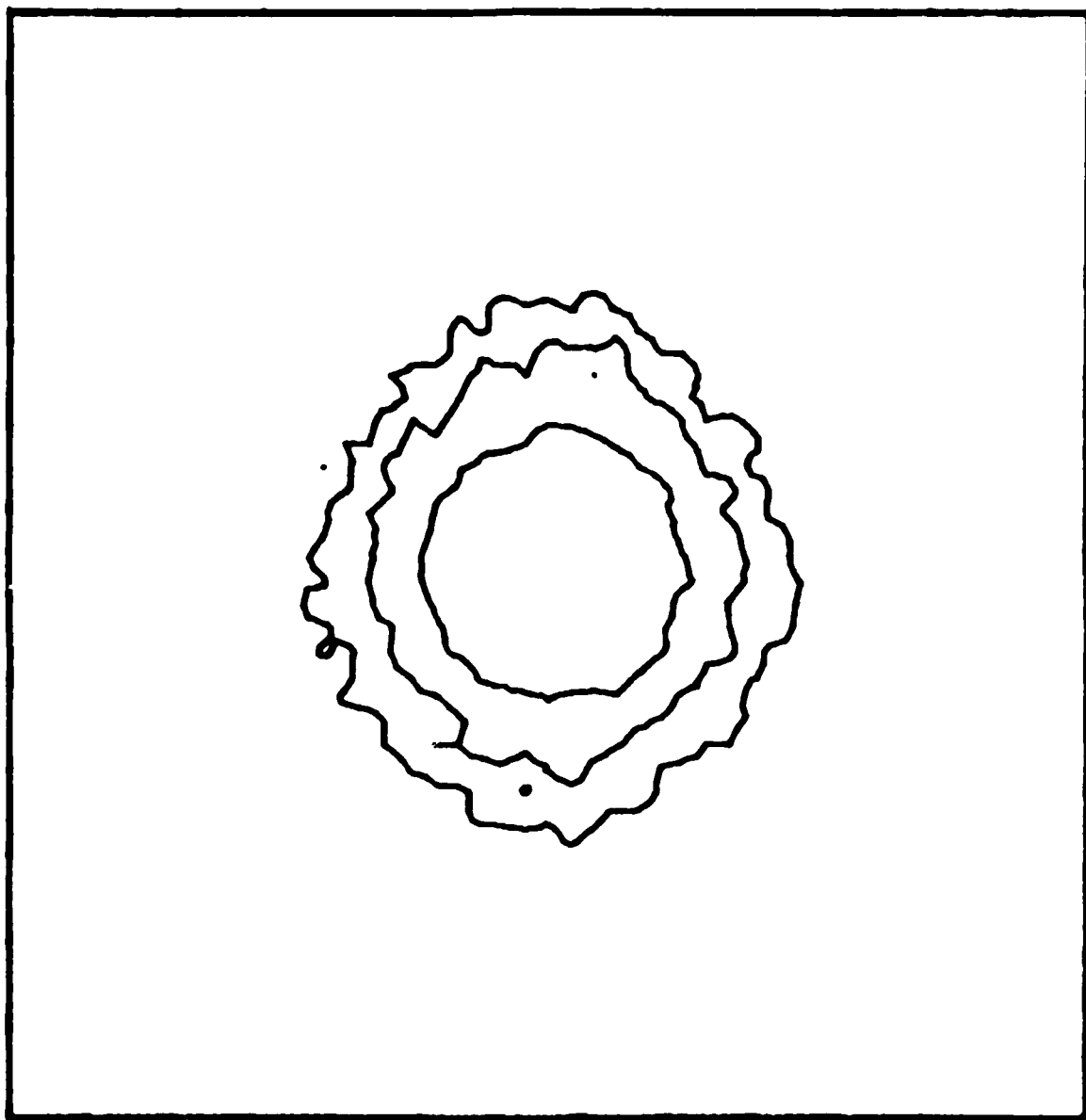


Fig. 21 -- A contour plot of the density in real space of the simulation with 30 degree depressed phase advance after 100 magnet pairs. The plot is taken midway between an x -focusing and y -focusing lens.

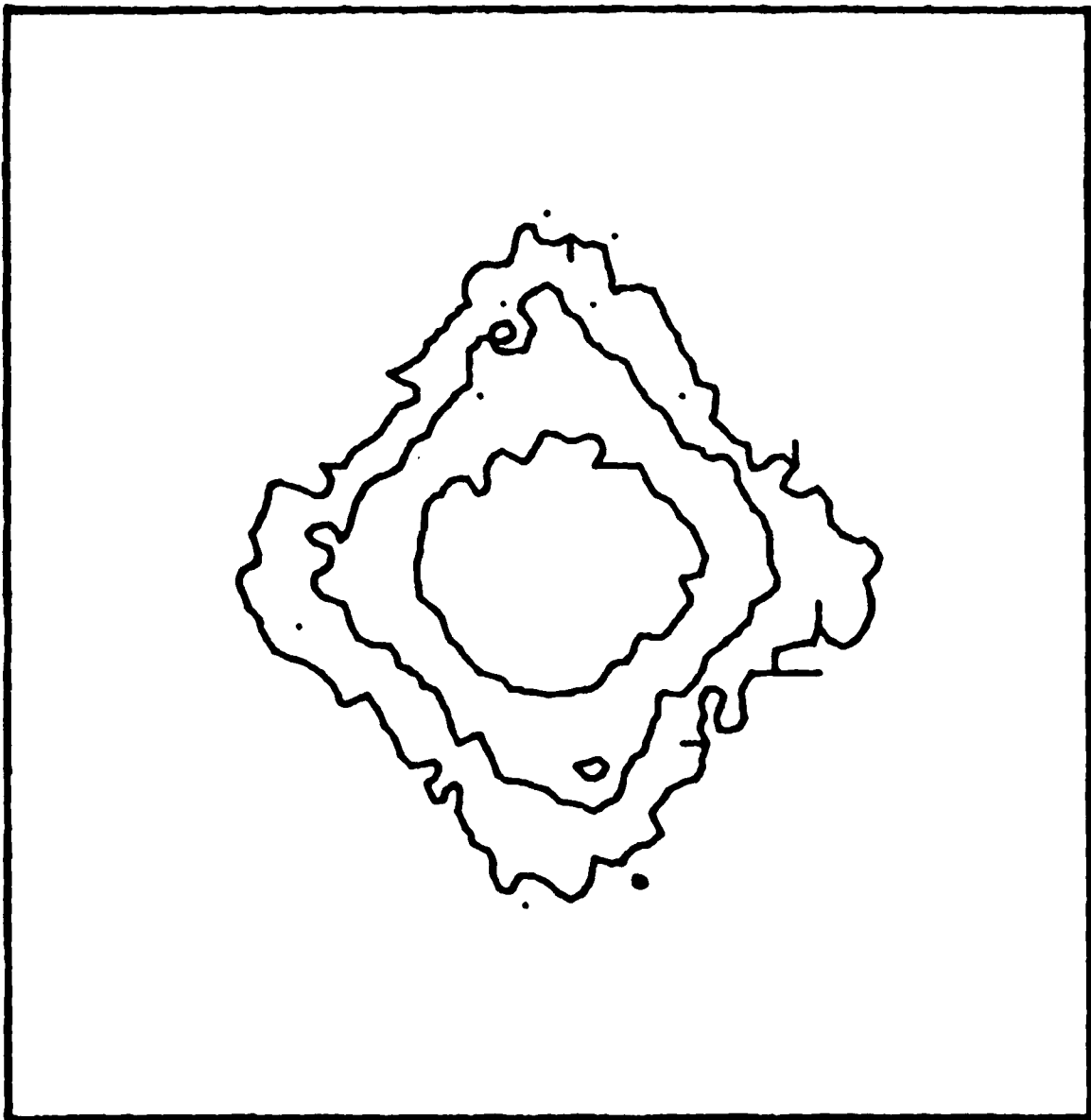


Fig. 22 — A contour plot of the density in momentum space at the same plane as Fig. 21

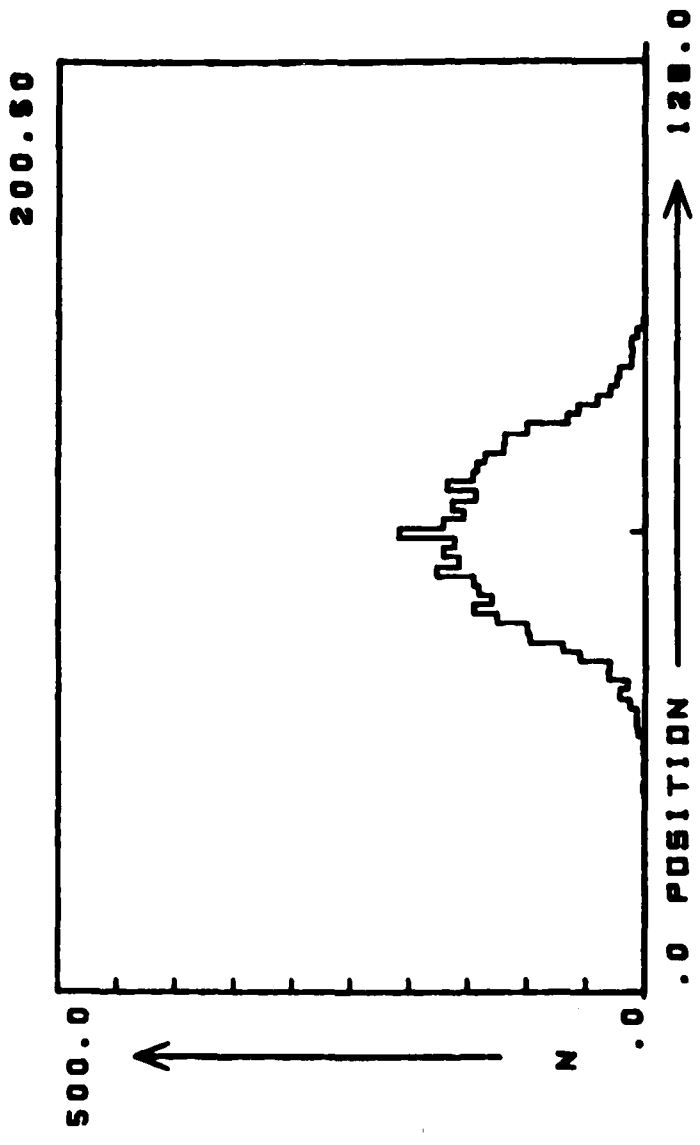


Fig. 23 - A plot of $f(x)$, the number density as a function of x , at the $y = 0$ plane, integrated over all the velocities. The plot is of the simulation with initial 30 degree depressed tune after traversing 100 magnet pairs, and is at the mid plane between two magnets

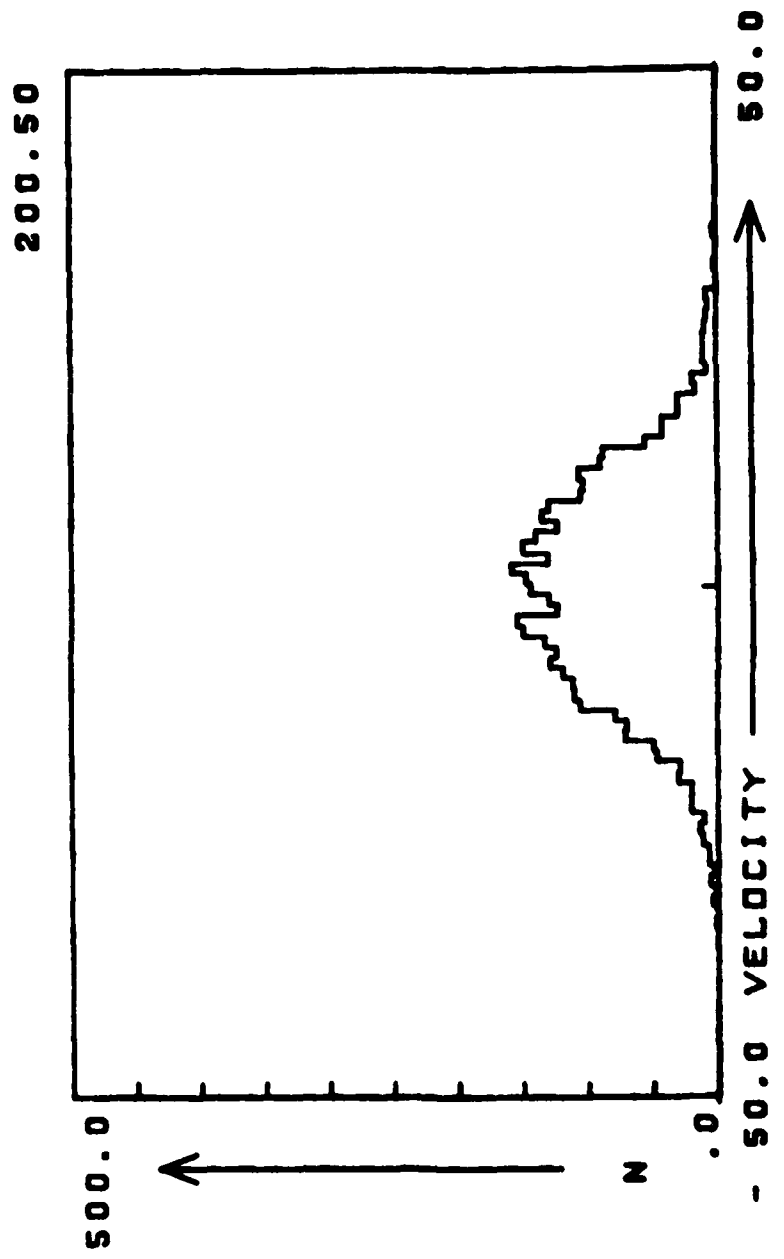


FIGURE 4 - A plot of $f(P_x)$ at $P_x = 0$ integrated over all positions at the midplane between two magnets

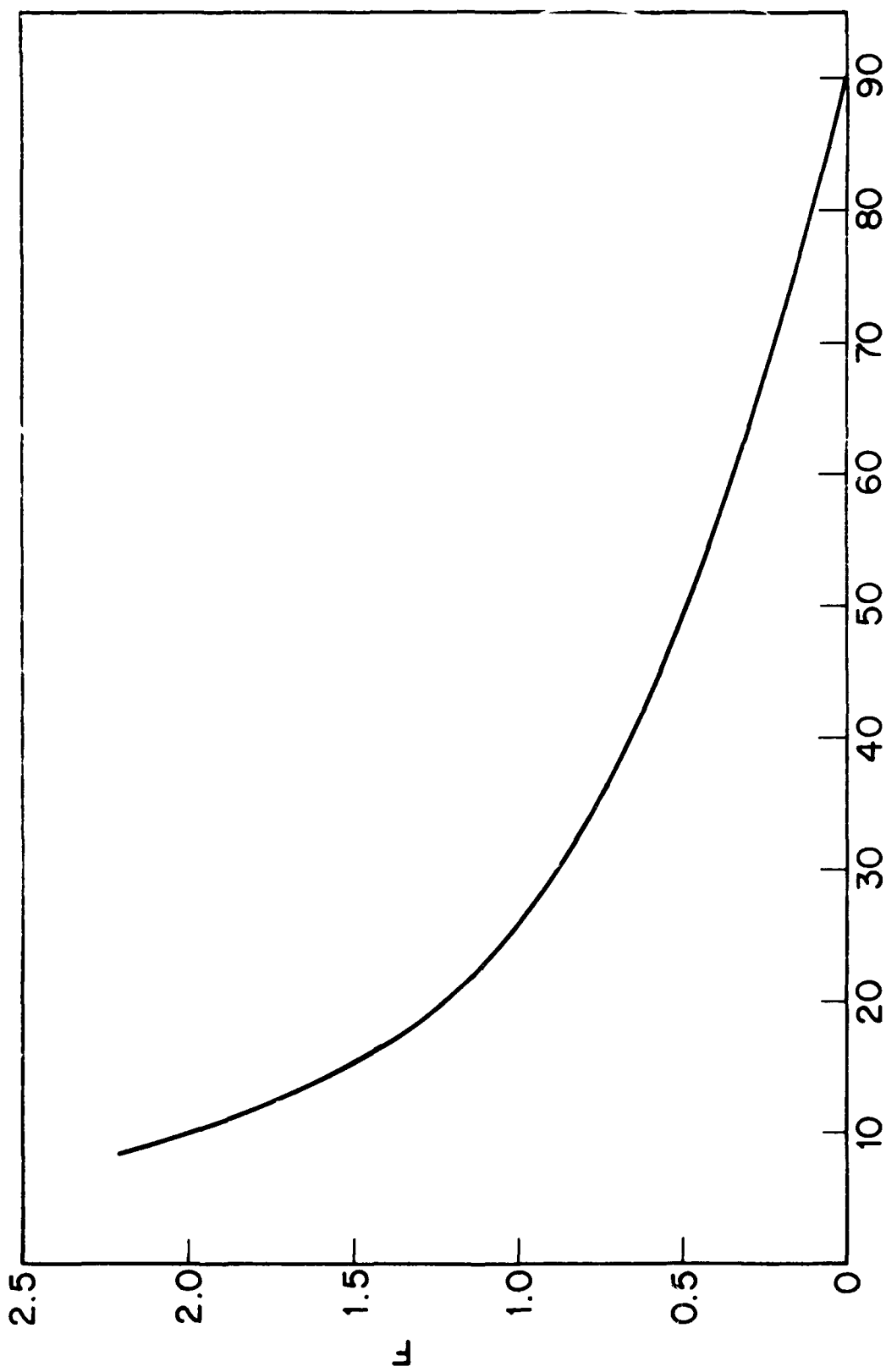


Fig. 8 - Plot of figure of merit, L , as a function of the dephased tune, σ , for a K.V. system with the lenses filter : one half of the longitudinal space

DISTRIBUTION LIST

U. S. Department of Energy
Washington, DC 20545

Mr. David Sutter, DOE Program Officer (2 copies)
Dr. Terry Godlove (Office of Inertial Fusion)

Naval Research Laboratory
Washington, DC 20375

I. Haber (Code 4790) (75 Copies)
Superintendent, Plasma Physics Div. Code 4700 (25 Copies)
Branch Head, Plasma Theory Branch Code 4790
Dr. Martin Lampe (Code 4790)
Dr. Stephen E. Bodner (Code 4730)

University of California
Lawrence Berkeley Laboratory
Berkeley, CA 94720

Dr. Denis Keefe
Dr. Lloyd Smith
Dr. L. J. Lasslett
Dr. A. Sessler
Dr. A. Sternlieb

Argonne National Laboratory
9700 South Cass Avenue
Argonne, IL 60439

Dr. Ronald L. Martin
Dr. S. Fenster
Dr. E. Colton

Accelerator Department
Associated Universities, Inc.
Brookhaven National Laboratory
Upton, NY 11973
Dr. A. W. Maschke

Los Alamos Scientific Laboratory
P. O. Box 1663
Los Alamos, NM 87545

Dr. George Sawyer
Dr. Lester E. Thode (MS-608)
Dr. Rickey J. Faehl (MS-608)
Dr. Richard K. Cooper (MS-808)
Dr. Larry Kennedy (MS-808)
Dr. R. Jameson (MS-820)

Lawrence Livermore Laboratory
P. O. Box 808
Livermore, CA 94550
Dr. F. W. Chambers (L-321)
Dr. Dave Bailey (L-477)
Dr. S. Yu
Dr. W. Barletta

National Bureau of Standards
Washington, DC 20234
Dr. S. Penner (Rad P B 102)

University of Maryland
College Park, MD 20742
Dr. M. Reiser
Dr. R. L. Gluckstern
Dr. Won Namkung

Stanford Linear Accelerator Center
Stanford University
P. O. Box 4349
Stanford, CA 94305
Dr. William B. Herrmannsfeldt

Mission Research Corporation
1400 San Mateo Blvd.
Albuquerque, NM 87108
Dr. Brendan B. Godfrey

Rutherford Laboratory
Chilton, Oxon
ENGLAND
Dr. M. King
Dr. J. D. Lawson

CANIL
Boite Postale #5027
14021 CAEN cedex
FRANCE
Dr. M. Prome
Dr. P. M. Lapostolle

CEN SACLAY
LNS BPn02
91180 GIF/YVETTE
FRANCE
Dr. J. L. Lemaire
Dr. J. L. Laclare

Institute fur Angewandte Physik
Universitet Frankfurt/Main
Robert-Mayer-Str. 2-4
D6000 Frankfurt/Main
WEST GERMANY
Dr. M. Deitinghoff

Max-Planck Institute for Plasma Physics
8046 Garching
WEST GERMANY
Dr. Ingo Hofmann

